Quantum geometry, non-adiabatic response and emergent macroscopic dynamics. Lecture notes. Karpacz Winter School, March 2014

Anatoli Polkovnikov[1]

[1] *Department of Physics, Boston University, Boston, MA 02215*

Contents

I. GAUGE POTENTIALS IN CLASSICAL AND QUANTUM HAMILTONIAN SYSTEMS.

A. Classical Hamiltonian systems.

Hamiltonian systems, are generally defined by specifying a set of canonical variables p_j, q_j satisfying canonical relations

$$\{p_i, q_j\} = \delta_{ij}, \tag{1}$$

where $\{\dots\}$ denotes the Poisson bracket:

$$\{A(\vec{p},\vec{q}), B(\vec{p},\vec{q})\} = \sum_j \frac{\partial A}{\partial p_j}\frac{\partial B}{\partial q_j} - \frac{\partial B}{\partial p_j}\frac{\partial A}{\partial q_j}. \tag{2}$$

It is easy to check that any orthogonal transformation

$$Q = R(\lambda)q,\ P = R(\lambda)p \tag{3}$$

preserves the Poisson bracket. A general class of transformations which preserve the Poisson brackets are known as canonical transformations and can be expressed through the generating functions (Landau and Lifshitz, 1982). It is easy to check that continuous canonical transformations can be generated by gauge potentials $\mathcal{A}_\lambda$:

$$q_j(\lambda + \delta\lambda) = q_j(\lambda) - \frac{\partial \mathcal{A}_\lambda(\lambda, \vec{p}, \vec{q})}{\partial p_j}\delta\lambda, \tag{4}$$

$$p_j(\lambda + \delta\lambda) = p_j(\lambda) + \frac{\partial \mathcal{A}_\lambda(\lambda, \vec{p}, \vec{q})}{\partial q_j}\delta\lambda, \tag{5}$$

where λ parametrizes the canonical transformation and the gauge potential is an arbitrary function of canonical variables and the parameter. Then up to terms of the order of $\delta\lambda^2$ the transformation above preserves the Poisson brackets

$$\{p_i(\lambda + \delta\lambda), q_j(\lambda + \delta\lambda)\} = \delta_{ij} + \delta\lambda\left(\frac{\partial^2 \mathcal{A}_\lambda}{\partial p_j \partial q_i} - \frac{\partial^2 \mathcal{A}_\lambda}{\partial p_j \partial q_i}\right) + O(\delta\lambda^2) = \delta_{ij} + O(\delta\lambda^2). \tag{6}$$

Exercises.

1. Show that the generator of translations $\vec{q}(X) = \vec{q}_0 - \vec{X}$ is the momentum operator: $\vec{\mathcal{A}}_{\vec{X}}(\vec{q}, \vec{p}) = \vec{p}$. You need to treat $\vec{X}$ as a three-component parameter $\vec{\lambda}$.

2. Show that the generator of rotations around z-axis:

$$q_x(\theta) = \cos(\theta)q_{x0} - \sin(\theta)q_{y0},\ q_y(\theta) = \cos(\theta)q_{y0} + \sin(\theta)q_{x0},$$

$$p_x(\theta) = \cos(\theta)p_{x0} - \sin(\theta)p_{y0},\ p_y(\theta) = \cos(\theta)p_{y0} + \sin(\theta)p_{x0},$$

   is the angular momentum operator: $\mathcal{A}_\theta = p_x q_y - p_y q_x$.

3. Find the gauge potential $\mathcal{A}_\lambda$ corresponding to the orthogonal transformation (3).

Hamiltonian dynamics is a particular canonical transformation parametrized by time

$$\frac{dq_j}{\partial t} = \{\mathcal{H}, q_j\} = \frac{\partial \mathcal{H}}{\partial p_j},\ \frac{dp_j}{\partial t} = \{\mathcal{H}, p_j\} = -\frac{\partial \mathcal{H}}{\partial q_j} \tag{7}$$

Clearly these Hamiltonian equations are equivalent to Eqs. (5) with the convention $\mathcal{A}_t = -\mathcal{H}$. This observation shows that the gauge potentials $\mathcal{A}_\lambda$ are generators of motion in the parameter space.

One can extend canonical transformations to the complex variables. Instead of doing this in full generality we will focus on particular phase space variables which are complex wave amplitudes. For example let us consider a system of harmonic oscillators which can be always described by the normal modes parameterized by k (for translationally invariant system k represents the momentum). Each mode is an independent harmonic oscillator described by the Hamiltonian:

$$\mathcal{H}_k = \frac{p_k^2}{2m} + \frac{m\omega_k^2}{2} q_k^2. \tag{8}$$

Let us define new linear combinations

$$p_k = i\sqrt{\frac{m\omega_k}{2}}(a_k^* - a_k),\ q_k = \sqrt{\frac{1}{2m\omega_k}}(a_k + a_k^*) \tag{9}$$

or equivalently

$$a_k^* = \frac{1}{\sqrt{2}}\left(q_k\sqrt{m\omega_k} - \frac{i}{\sqrt{m\omega_k}}p_k\right),\ a_k = \frac{1}{\sqrt{2}}\left(q_k\sqrt{m\omega_k} + \frac{i}{\sqrt{m\omega_k}}p_k\right). \tag{10}$$

Next we compute the Poisson brackets of the complex wave amplitudes

$$\{a_k, a_k\} = \{a_k^*, a_k^*\} = 0,\ \{a_k, a_k^*\} = i. \tag{11}$$

To avoid dealing with the imaginary Poisson brackets it is convenient to introduce new coherent state Poisson brackets

$$\{A, B\}_c = \sum_k \frac{\partial A}{\partial a_k}\frac{\partial B}{\partial a_k^*} - \frac{\partial B}{\partial a_k}\frac{\partial A}{\partial a_k^*}. \tag{12}$$

From this definition it is immediately clear that

$$\{a_k, a_q^*\}_c = \delta_{kq}. \tag{13}$$

Comparing this relation with Eq. (11) we see that standard and coherent Poisson brackets differ by the factor of i:

$$\{\dots\} = i\{\dots\}_c. \tag{14}$$

Infinitesimal canonical transformations preserving the coherent state Poisson brackets can be also defined using the guage potentials:

$$i\frac{\partial a_k}{\partial \lambda} = -\frac{\partial \mathcal{A}_\lambda}{\partial a_k^*},\quad i\frac{\partial a_k^*}{\partial \lambda} = \frac{\partial \mathcal{A}_\lambda}{\partial a_k}. \tag{15}$$

Exercise

- Check that any unitary transformation $\tilde{a}_k = U_{k,k'} a'_k$, where U is a unitary matrix, preserves the coherent state Poisson bracket, i.e. $\{\tilde{a}_k, \tilde{a}^*_q\}_c = \delta_{k,q}$. Verify that the Bogoliubov transformation

$$\gamma_k = \cosh(\theta_k) a_k + \sinh(\theta_k) a^*_{-k},\ \gamma^*_k = \cosh(\theta_k) a^*_k + \sinh(\theta_k) a_{-k}, \tag{16}$$

with $\theta_k = \theta_{-k}$ also preserves the coherent state Poisson bracket, i.e.

$$\{\gamma_k, \gamma_{-k}\}_c = \{\gamma_k, \gamma^*_{-k}\}_c = 0,\ \{\gamma_k, \gamma^*_k\}_c = \{\gamma_{-k}, \gamma^*_{-k}\}_c = 1. \tag{17}$$

Assume that θ_k are known functions of some parameter λ, e.g. the interaction strength. Find the gauge potential $\mathcal{A}_\lambda = \sum_k \mathcal{A}_k$, which generates such transformations.

We can write the Hamiltonian equations of motion for the new coherent variables. Using that

$$\frac{da}{dt} = \frac{\partial a}{\partial t} - \{a, \mathcal{H}\} = \frac{\partial a}{\partial t} - i\{a, \mathcal{H}\}_c \tag{18}$$

and using that our variables do not explicitly depend on time (such dependence would amount to going to a moving frame, which we will discuss later) we find

$$i\frac{da_k}{dt} = \{a_k, \mathcal{H}\}_c = \frac{\partial \mathcal{H}}{\partial a^*_k},\ i\frac{da^*_k}{dt} = \{a^*_k, \mathcal{H}\}_c = -\frac{\partial \mathcal{H}}{\partial a_k} \tag{19}$$

These equations are also known as Gross-Pitaevskii equations. Note that these equations are arbitrary for arbitrary Hamiltonians and not restricted to harmonic systems.

And finally let us write down the Liouville equations of motion for the probability distribution $\rho(q, p, t)$ or $\rho(a, a^*, t)$. The latter just express incompressibility of the probability fllow, which directly follows conservation of the phase space volume $d\Gamma = dqdp$ or $d\Gamma = dada^*$ for arbitrary canonical transformations including time evolution and from the conservation of the total probability $\rho d\Gamma$:

$$0 = \frac{d\rho}{dt} = \frac{\partial \rho}{\partial t} - \{\rho, H\} = \frac{\partial \rho}{\partial t} - i\{\rho, H\}_c, \tag{20}$$

or equivalently

$$\frac{\partial \rho}{\partial t} = \{\rho, H\},\ i\frac{\partial \rho}{\partial t} = -\{\rho, H\}_c \tag{21}$$

B. Quantum Hamiltonian systems.

An analogue of canonical transformations in classical mechanics are unitary transformations in quantum mechanics. In classical systems these transformations reflect the freedom of choosing canonical variables while in quantum systems they reflect the freedom of choosing basis states.

The wave function representing some state can be always expanded in some basis:

$$|\psi\rangle = \sum_n \psi_n |n\rangle_0, \tag{22}$$

where $|n\rangle_0$ is some fixed, parameter independent basis. One can always make a unitary transformation to some other basis $|n(\lambda)\rangle = U_{nm}(\lambda)|n_0\rangle$ or equivalently $|n_0\rangle = U^*_{nm}|m(\lambda)\rangle$.[1] Then the same state $|\psi\rangle$ can be written as

$$|\psi\rangle = \sum_n \psi_n U^*_{nm}|m(\lambda)\rangle = \sum_m \tilde{\psi}_m(\lambda)|m(\lambda)\rangle, \tag{23}$$

where $\tilde{\psi}_m(\lambda) = U^*_{nm}\psi_n = U^\dagger\psi$. We can introduce gauge potentials by analogy with the classical systems as generators of continuous unitary transformations. Namely

$$i\partial_\lambda\tilde{\psi}(\lambda) = -iU^\dagger\partial_\lambda U U^\dagger\psi = -iU^\dagger\partial_\lambda U\tilde{\psi} = -\mathcal{A}_\lambda\tilde{\psi}, \tag{24}$$

where we introduced the guage potential

$$\mathcal{A}_\lambda = iU^\dagger\partial_\lambda U. \tag{25}$$

Note that up to the sign the gauge potential plays the role similar to the Hamiltoninan, i.e. it generates the motion in the parameter space. It is easy to check that the gauge potential is a Hermitian operator

$$\mathcal{A}^\dagger_\lambda = i\partial_\lambda U^\dagger U = \mathcal{A}_\lambda, \tag{26}$$

where we used that

$$\partial_\lambda U^\dagger = -U^\dagger\,\partial_\lambda U\,U^\dagger. \tag{27}$$

The gauge potential can be also represented through the matrix elements:

$$\langle n_0|\mathcal{A}_\lambda|m_0\rangle = i\langle n_0|U^\dagger\partial_\lambda U|m_0\rangle = i\langle n(\lambda)|\partial_\lambda|m(\lambda)\rangle. \tag{28}$$

or equivalently

$$\mathcal{A}_\lambda = i\partial_\lambda. \tag{29}$$

We work in units where $\hbar = 1$, otherwise it is more appropriate to define $\mathcal{A}_\lambda = i\hbar\partial_\lambda$. The diagonal elements of the gauge potentials in the basis of some Hamiltonian $\mathcal{H}(\lambda)$ are the Berry connections,

[1] Unless otherwise specified we always imply summation over repeated indices.

which we will discuss in detail later. So the Berry connections are direct analogues of energies representing the expectation values of the gauge potentials. With this definition one can extend the notion of the Berry connections to arbitrary states.

Exercises

1. Verify that the gauge potential corresponding to the translations: $\tilde{\psi}(x) = \psi(\lambda + x)$ is the momentum operator. Similarly verify that the gauge potential for rotations is the angular momentum operator.

2. Consider the quantum version of the Bogoliubov transformations discussed in the previous section (Eq. (16)). Show that the quantum and classical gauge potentials coincide if we identify complex amplitudes a_k and a_k^* with the annihilation and creation operators respectively.

C. Hamiltonian dynamics in the moving frame. Galilean transformation.

Gauge potentials are closely integrated into the Hamiltonian dynamics. In particular, they naturally appear in gauge theories like electromagnetism to enforce the gauge invariance. We will come to this issue later. For now we simply note that the equations of motion should be invariant under the gauge transformations. Indeed we can describe the same system using an arbitrary set of canonical variables in the classical language or an arbitrary basis in the quantum language.

Let us consider now the classical equations of motion of some system described by the Hamiltonian, possibly time and parameter dependent (the system can be either single- or many- particle). For the parameter-independent canonical variables the equations of motion are

$$\frac{dq}{dt} = \{\mathcal{H}, q\},\ \frac{dp}{dt} = \{\mathcal{H}, p\} \tag{30}$$

Now let us go to the moving frame, i.e. let us find the analogous equations of motion in terms of canonical variables $q(\lambda, t)$, $p(\lambda, t)$. Then obviously

$$\frac{dq}{dt} = \frac{\partial q}{\partial t} + \dot{\lambda}\frac{\partial q}{\partial \lambda}. \tag{31}$$

Note that $d_t q$ is the full derivative in the moving frame, while $\partial_t q$ is the derivative in the lab frame where the definition of q does not depend on λ and thus it is described by Eqs. (30). Using the definition of the gauge potential we find

$$\frac{dq}{dt} = \{\mathcal{H}, q\} - \dot{\lambda}\{\mathcal{A}_\lambda, q\},\ \frac{dp}{dt} = \{\mathcal{H}, p\} - \dot{\lambda}\{\mathcal{A}_\lambda, p\}. \tag{32}$$

We thus see that the equations of motion in the moving frame preserve their Hamiltonian nature. The new moving Hamiltonian is given by the generalized Galilean transformation

$$\mathcal{H}_m = \mathcal{H} - \dot{\lambda}\mathcal{A}_\lambda. \tag{33}$$

If λ stands for a say x-coordinate of the reference frame then as we discussed $\mathcal{A}_\lambda = P_x$ and the expression above reduces to the standard Galilean transformation. If λ stands for an angle of the reference frame that $\mathcal{A}_\lambda$ is the angular momentum and the transformation of the Hamiltonian reduces to the Hamiltonian in the rotating frame, if λ is the dilation parameter then

$$\mathcal{H}_m = \mathcal{H} - \frac{\dot{\lambda}}{\lambda}\sum_j q_j p_j. \tag{34}$$

Similarly one can check that standard gauge transformations in electromagnetism can be also understood through going to a moving frame with respect to momentum.

Exercise

- Find the gauge potential corresponding to the translations of the momentum $p = p + \lambda(t)$. Find the gauge potential describing this transformation. Show that the moving frame Hamiltonian with the Galilean term accounts to the standard gauge transformation in the electromagnetism where $A_x \to A_x + \partial_q f,\ \varphi \to \varphi - \partial_t f$, where A_x and φ are the x-component of the vector potential and the scalar potential. Find the relation between the guage potential and the function f.

It is interesting that the Galilean transformation can be understood from the extended variational principle, where the equations of motion can be obtained by extremizing the action in the extended parameter space-time

$$S = \int [p\, dq - \mathcal{H}dt + \mathcal{A}_\lambda d\lambda] \tag{35}$$

with respect to all possible trajectories $p(\lambda, t)$, $q(\lambda, t)$ satisfying the initial conditions. Extremizing the action at constant time t clearly gives back the canonical transformations (5). Extremizing this action with respect to time reproduces the Hamiltonian equations of motion. If we extremize the action along some space time trajectory $\lambda(t)$ such that $d\lambda = \dot{\lambda}dt$ we will clearly reproduce the Hamiltonian equations of motion with the Galilean term (33).

Very similar analysis goes through for the quantum systems. Thus the Schroedinger equation

$$i\partial_t \psi = \mathcal{H}\psi \tag{36}$$

after the transformation to the moving frame: $\psi = U(\lambda)\tilde{\psi}$ reads

$$i\dot{\lambda}(\partial_\lambda U)\tilde{\psi} + iU\partial_t\tilde{\psi} = \mathcal{H}U\tilde{\psi} \tag{37}$$

Multiplying both sides of this equation by $U^\dagger$ and moving the first term in the L.H.S. of this equation to the right we find

$$i\partial_t\tilde{\psi} = \left[U^\dagger\mathcal{H}U - \dot{\lambda}\mathcal{A}_\lambda\right]\tilde{\psi}. \tag{38}$$

Here $U^\dagger\mathcal{H}U$ is the original Hamiltonian written in the rotating basis while $-\dot{\lambda}\mathcal{A}_\lambda$ is the Galilean term.

To be more specific let us consider a simple example of a spin one half particle in an external field. The Hamiltonian in the fixed (lab) frame is:

$$\mathcal{H}(\lambda) = -\Delta\left(\cos(\lambda)\,\sigma_z + \sin(\lambda)\,\sigma_x\right)$$

with eigenstates

$$|gs_\lambda\rangle = \begin{pmatrix} \cos\left(\frac{\lambda}{2}\right) \\ \sin\left(\frac{\lambda}{2}\right) \end{pmatrix}, \quad |ex_\lambda\rangle = \begin{pmatrix} -\sin\left(\frac{\lambda}{2}\right) \\ \cos\left(\frac{\lambda}{2}\right) \end{pmatrix}$$

We will consider a very specific unitary transformation, which will be very important throughout this course, namely the transformation, which diagonalizes the instantaneous Hamiltonian, $\mathcal{H}(\lambda)$. Clearly this transformation is simply the rotation around the y-axis λ:

$$U(\lambda) = \exp\left[-i\frac{\sigma_y}{2}\lambda\right] = \begin{pmatrix} \cos(\lambda/2) & -\sin(\lambda/2) \\ \sin(\lambda/2) & \cos(\lambda/2) \end{pmatrix}$$

Note that $U(\lambda_0 = 0) = I$ is the identity matrix. Then the gauge potential is:

$$\mathcal{A}_\lambda = iU^\dagger(\lambda)\left(\partial_\lambda U(\lambda)\right) = \frac{\sigma_y}{2},$$

which in this example is λ-independent. Note that the Pauli matrix σ_y acts in the basis of the instantaneous Hamiltonian.

$$\tilde{H} \equiv U^\dagger(\lambda)\mathcal{H}(\lambda)U(\lambda) = -\Delta\sigma_z,$$

with the eigenstates

$$|\tilde{gs}\rangle = \begin{pmatrix} 1 \\ 0 \end{pmatrix}, \quad |\tilde{ex}\rangle = \begin{pmatrix} 0 \\ 1 \end{pmatrix}.$$

By direct inspection one can verify that

$$\frac{1}{2}\langle\tilde{n}|\sigma_y|\tilde{m}\rangle = i\langle n|\partial_\lambda|m\rangle, \tag{39}$$

where $n, m = \{gs, es\}$.

II. GEOMETRY OF THE GROUND STATE MANIFOLD. FUBINI-STUDY METRIC AND THE BERRY CURVATURE.

In the previous section we treated quantum and classical systems on equal footing. In this section we will focus on the geometric properties of the ground state manifold thus will focus on exclusively quantum systems. In the next section, where we will study relation between geometry and dynamics we will again consider both classical and quantum systems.

The first notion of the quantum geometric tensor appeared in 1980 in Ref. (Provost and Vallee, 1980). Formally the geometric tensor is defined on any manifold of states characterized by some parameter $\vec{\lambda}$: $|\psi_0(\vec{\lambda})\rangle$.[2] We will be interested in the family of ground states of some Hamiltonian $\mathcal{H}(\vec{\lambda})$. We will assume that the ground state is either non-degenerate or in the case of degeneracy ground states are not connected by the matrix elements of generalized forces $\partial_{\lambda_\alpha}\mathcal{H}$. The geometric tensor naturally appears when one considers the distance between nearby states $|\psi_0(\vec{\lambda})\rangle$ and $|\psi_0(\vec{\lambda}+\delta\vec{\lambda})\rangle$ and expands it to the lowest order in $\delta\vec{\lambda}$:

$$d \equiv 1 - f^2 = 1 - |\langle\psi_0(\vec{\lambda})|\psi_0(\vec{\lambda}+\delta\vec{\lambda})\rangle|^2, \tag{40}$$

where $f = |\langle\psi_0(\vec{\lambda})|\psi_0(\vec{\lambda}+\delta\vec{\lambda})\rangle|$ is the so called fidelity of the ground state. Note that $1-f^2$ is always positive therefore at small $\delta\vec{\lambda}$ the Taylor expansion of this quantity should not contain any first order terms in $\delta\vec{\lambda}$ and rather start with a quadratic term:

$$1 - f^2 = \delta\lambda_\alpha \chi_{\alpha\beta} \delta\lambda_\beta + O(|\delta\vec{\lambda}|^3), \tag{41}$$

where $\chi_{\alpha\beta}$ is the symmetric positive definite geometric tensor. To find this tensor explicitly let us note that $1-f^2$ is nothing but the probability to excite the system during a quantum quench where the parameter suddenly changes from $\vec{\lambda}$ to $\vec{\lambda}+\delta\vec{\lambda}$. Indeed f^2 is simply the probability to remain in the ground state after this quench. The amplitude of going to the excited state is

$$a_n = \langle\psi_n(\vec{\lambda}+\delta\vec{\lambda})|\psi_0(\vec{\lambda})\rangle \approx \delta\lambda_\alpha \langle n|\overleftarrow{\partial}_\alpha|0\rangle, \tag{42}$$

where to shorten the notations we introduced $\partial_\alpha \equiv \partial_{\lambda_\alpha}$ and the arrow over the derivative indicates that it acts on the left. Also to simplify notations we use $|n\rangle$ instead of $|\psi_n(\vec{\lambda})\rangle$. Differentiating the orthonormality condition $\langle n|m\rangle$ with respect to λ_α we find

$$\langle n|\overleftarrow{\partial}_\alpha|m\rangle + \langle n|\partial_\alpha|m\rangle = 0. \tag{43}$$

[2] From now on we will assume that the parameters can be multi-component.

Recall that (see Eq. (28))

$$i\langle n|\partial_\alpha|m\rangle = \langle\tilde{n}|\mathcal{A}_\alpha|\tilde{m}\rangle, \tag{44}$$

where tilde refers to the instantaneous basis, i.e. the basis at $\vec{\lambda}+\delta\vec{\lambda}$. Thus we see that the amplitude of going to the excited state in the leading order in $\delta\vec{\lambda}$ is given essentially by the matrix element of the gauge potential

$$a_n = \delta\lambda_\alpha\langle n|\overleftarrow{\partial}_\alpha|0\rangle = -\delta\lambda_\alpha\langle n|\partial_\alpha|0\rangle + O(|\delta\vec{\lambda}|^2) = i\langle n|\mathcal{A}_\alpha|0\rangle + O(|\delta\vec{\lambda}|^2). \tag{45}$$

Note that we can skip the tilde in the basis because in the leading order in $\delta\vec{\lambda}$ the basis does not change. Thus we see that

$$1-f^2 = \sum_{n\neq 0}|a_n^2| = \sum_{n\neq 0}\delta\lambda_\alpha\delta\lambda_\beta\langle 0|\mathcal{A}_\alpha|n\rangle\langle n|\mathcal{A}_\beta|0\rangle + O(|\delta\vec{\lambda}|^3) = \delta\lambda_\alpha\delta\lambda_\beta\langle 0|\mathcal{A}_\alpha\mathcal{A}_\beta|0\rangle_c + O(|\delta\vec{\lambda}|^3), \tag{46}$$

where the subindex c implies that we are taking the connected correlation function (or equivalently the covariance):

$$\langle 0|\mathcal{A}_\alpha\mathcal{A}_\beta|0\rangle_c = \langle 0|\mathcal{A}_\alpha\mathcal{A}_\beta|0\rangle - \langle 0|\mathcal{A}_\alpha|0\rangle\langle 0|\mathcal{A}_\beta|0\rangle. \tag{47}$$

This covariance precisely determines the geometric tensor introduced by Provost and Vallee

$$\chi_{\alpha\beta} = \langle 0|\mathcal{A}_\alpha\mathcal{A}_\beta|0\rangle_c. \tag{48}$$

In terms of many-body wave functions the geometric tensor can be expressed through the overlap of derivatives:

$$\chi_{\alpha\beta} = \langle 0|\overleftarrow{\partial}_\alpha\partial_\beta|0\rangle_c = \langle\partial_\alpha\psi_0|\partial_\beta\psi_0\rangle_c = \langle\partial_\alpha\psi_0|\partial_\beta\psi_0\rangle - \langle\partial_\alpha\psi_0|\psi_0\rangle\langle\psi_0|\partial_\beta\psi_0\rangle. \tag{49}$$

The last term in this expression is necessary to enforce invariance of the distance under arbitrary global phase transformations of the wave function $\psi_0(\vec{\lambda}) \to \exp[i\phi(\vec{\lambda})]\psi_0(\vec{\lambda})$, which should not affect the notion of the distance between different ground states.

Note that in general the geometric tensor is not symmetric. Indeed because the operators $\mathcal{A}_\alpha$ are Hermitian one can show that

$$\chi_{\alpha\beta} = \chi^*_{\beta\alpha}. \tag{50}$$

Only the symmetric part of $\chi_{\alpha\beta}$ determines the distance between the states. Indeed in the quadratic form

$$d = \delta\lambda_\alpha\chi_{\alpha\beta}\delta\lambda_\beta \tag{51}$$

one can always symmetrize the indexes α and β so that the antisymmetric part drops out. Nevertheless, as we will see shortly, both the symmetric and the anti-symmetric parts of the geometric tensor are very important so we will introduce both

$$g_{\alpha\beta} = \frac{\chi_{\alpha\beta} + \chi_{\beta\alpha}}{2} = \frac{1}{2}\langle 0|\mathcal{A}_\alpha\mathcal{A}_\beta + \mathcal{A}_\beta\mathcal{A}_\alpha|0\rangle = \Re\langle 0|\mathcal{A}_\alpha\mathcal{A}_\beta|0\rangle \tag{52}$$

is called the Fubini-Study metric tensor.[3] The imaginary part of the geometric tensor is known as the Berry curvature (Berry, 1984). It plays a crucial role in most known quantum topological phenomena:

$$F_{\alpha\beta} = i(\chi_{\alpha\beta} - \chi_{\beta\alpha}) = -2\Im\chi_{\alpha\beta} = i\langle 0|[\mathcal{A}_\alpha, \mathcal{A}_\beta]|0\rangle. \tag{53}$$

Let us note that the Berry curvature can be expressed through the derivatives of the Berry connections:

$$F_{\alpha\beta} = \partial_\alpha A_\beta - \partial_\beta A_\alpha, \tag{54}$$

where

$$A_\alpha = \langle 0|\mathcal{A}_\alpha|0\rangle = i\langle 0|\partial_\alpha|0\rangle. \tag{55}$$

Indeed direct differentiation gives

$$\partial_\alpha A_\beta - \partial_\beta A_\alpha = i\langle 0|\overleftarrow{\partial}_\alpha\partial_\beta|0\rangle - i\langle 0|\overleftarrow{\partial}_\beta\partial_\alpha|0\rangle + i\langle 0|\partial^2_{\alpha\beta}|0\rangle - i\langle 0|\partial^2_{\beta\alpha}|0\rangle = i(\chi_{\alpha\beta} - \chi_{\beta\alpha}). \tag{56}$$

The Berry connection is directly related to the phase of the ground state wave function. Indeed representing the latter as

$$\psi_0 = |\psi_0|\exp[i\phi] \tag{57}$$

we find that

$$A_\alpha = -\partial_\alpha\phi \tag{58}$$

Therefore the integral of A_α over a closed path represents the total phase (Berry phase) accumulated by the wave function during the adiabatic evolution

$$\gamma = \oint_{\vec{l}}\partial_\alpha\phi d\lambda_\alpha = -\oint_{\vec{l}} A_\alpha d\lambda_\alpha \tag{59}$$

[3] Sometimes in literature by the Fubini-Study metric one understands the complete metric in the projective Hilbert space where the number of parameters λ_α coincides with the dimension of the Hilbert space.

By the Stokes theorem the same phase can be represented as the integral of the Berry curvature over the surface enclosed by the contour $\vec{l}$:

$$\gamma = \int_S F_{\alpha\beta} d\lambda_\alpha \wedge d\lambda_\beta, \tag{60}$$

where the wedge product implies that the integral is directed.

To get an intuition about the Berry curvature and then the metric tensor let us consider two simple examples. First, following the original paper by Berry, let us consider the Aharonov-Bohm geometry, namely a particle confined in a deep potential in the presence of a solenoid. The Hamiltonian for this system is

$$\mathcal{H} = \frac{\left(\vec{p} - \frac{e}{c}\vec{\Lambda}(\vec{r})\right)^2}{2m} + V(\vec{r} - \vec{R}), \tag{61}$$

where $\vec{\Lambda}$ is the vector potential (we use $\vec{\Lambda}$ to avoid the confusion with the Berry connection) and $V(\vec{r}-\vec{R})$ is a confining potential near some point $\vec{R}$ outside the solenoid, where there is no magnetic field. Therefore the vector potential can be written as a gradient of the magnetic potential

$$\vec{\Lambda} = \vec{\nabla}\Phi \Rightarrow \Phi = \int \vec{\Lambda} d\vec{l}$$

Note that this expression is valid even if the magnetic field is non-zero but then the potential Φ is path dependent. It is well known that the vector potential can be eliminated by a gauge transformation:

$$\psi = \tilde{\psi} \exp\left[i\frac{e}{c\hbar}\Phi\right]. \tag{62}$$

Then the Hamiltonian for $\tilde{\psi}$ becomes independent of the vector potential and thus the wave function $\tilde{\psi}$ can be chosen to be real. In this case the Berry connection with respect to $\vec{R}$, the position of the trap, is

$$-\partial_{\vec{R}}\phi = -\frac{e}{c\hbar}\partial_{\vec{R}}\Phi = \frac{e}{c\hbar}\partial_{\vec{r}}\Phi = \frac{e}{c\hbar}\vec{\Lambda}(\vec{R}) \tag{63}$$

In general one needs to average the vector potential over the wave function $\tilde{\psi}(\vec{r})$ but assuming that it is localized near $\vec{R}$ the averaging is not important. So we see that up to fundamental constants the Berry connection plays the role of the vector potential, hence the Berry phase assumes the role of the flux and the Berry curvature (curl of the Berry connection) plays the role of the magnetic field. This analogy is very useful when we think about general parameter space and as we will see later this analogy is not coincidental. Like the magnetic field the Berry curvature is the source of the Lorentz force.

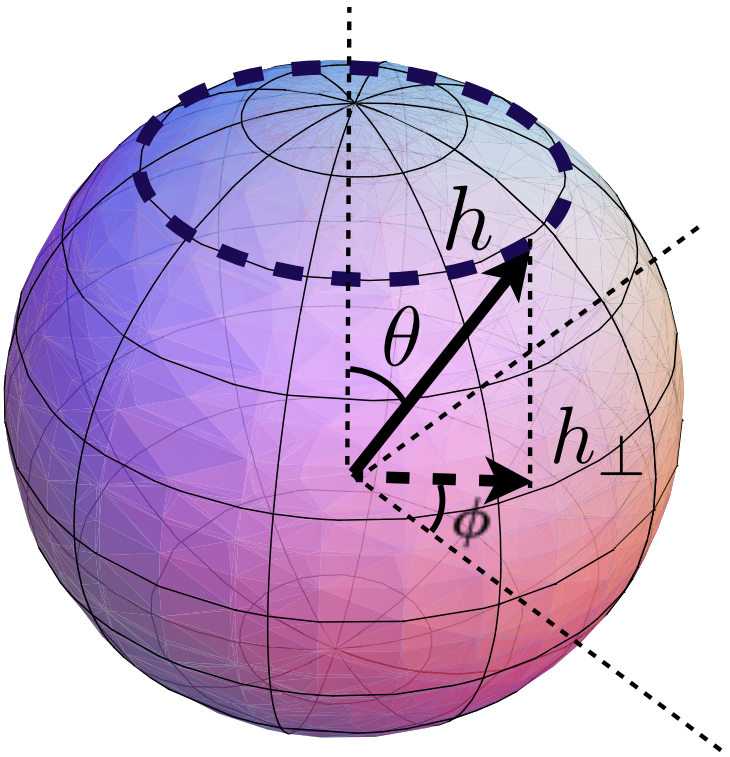

FIG. 1 Schematic representation of the spin in an external magnetic field, where the angles of the magnetic field θ and ϕ are the parameters.

Now let us consider the next illustrative example of a spin one half in an external magnetic field. We will analyze the geometry shown in Fig. 1. The Hamiltonian of this system is

$$\mathcal{H} = -\vec{h}\vec{\sigma}. \tag{64}$$

Because the ground state does not depend on the magnitude of the magnetic field we can choose parameters to be the angles θ and ϕ. We already discussed the ground and excited states for this model at $\phi = 0$. For general ϕ we have

$$|\psi_0\rangle = \begin{pmatrix} \cos(\theta/2)\mathrm{e}^{i\phi/2} \\ \sin(\theta/2)\mathrm{e}^{-i\phi/2} \end{pmatrix}, \quad |\psi_1\rangle = \begin{pmatrix} -\sin(\theta/2)\mathrm{e}^{i\phi/2} \\ \cos(\theta/2)\mathrm{e}^{-i\phi/2} \end{pmatrix}.$$

Direct evaluation of the geometric tensor for the ground state gives

$$\chi_{\theta\theta} = \frac{1}{4},\ \chi_{\phi\phi} = \frac{1}{4}\sin^2(\theta),\ \chi_{\theta\phi} = -\frac{i}{4}\sin(\theta) \tag{65}$$

This expressions can be either computed by direct differentiation of the ground state wave function with respect to θ and ϕ or from calculating the covariance matrix of the gauge potentials

$$\mathcal{A}_\theta = i\partial_\theta = \frac{1}{2}\tau_y,\ \mathcal{A}_\phi = i\partial_\phi = \frac{1}{2}(\cos(\theta)\tau_z + \sin(\theta)\tau_x) \tag{66}$$

Recall that the Pauli matrices here act in the basis of instantaneous eigenstates where the Hamiltonian is $\mathcal{H} = -h\tau_z$. The equations above generalize to particles with arbitrary spin where instead of spin one half operators like $1/2\tau_y$ one uses the angular momentum operators like S_y.

From the expression for the geometric tensor we see that the nonzero metric tensor components are

$$g_{\theta\theta} = \frac{1}{4},\ g_{\phi\phi} = \frac{1}{4}\sin^2\theta, \tag{67}$$

and the Berry curvature is

$$F_{\theta\phi} = \frac{1}{2}\sin(\theta). \tag{68}$$

Note that the Fubini-Study metric for this model is equivalent to the metric of a sphere of radius $r = 1/2$. It is interesting to point that for the excited state the metric tensor is the same while the Berry curvature has an opposite sign.

Originally Provost and Vallee thought that the metric tensor is a nice mathematical object, which is however unmeasurable. Contrary it was immediately understood that the Berry curvature is responsible for many different physical phenomena like the Aharonov-Bohm effect or the quantum Hall effect. Later in the course we will discuss in a greater detail the relation between the geometric tensor and the dynamical response. For now let us show that the geometric tensor is measurable and related to the standard dynamical response coefficients. Indeed let us differentiate the relation

$$\mathcal{H}|n\rangle = E_n|n\rangle \tag{69}$$

with respect to λ and multiply both sides on $\langle m|$, where $m \neq n$. For simplicity we will assume there are no degeneracies. Then we find

$$\langle m|\partial_\lambda\mathcal{H}|n\rangle + E_m\langle m|\partial_\lambda|n\rangle = E_n\langle m|\partial_\lambda|n\rangle.$$

Thus we find

$$\langle m|\partial_\lambda|n\rangle = \frac{\langle m|\partial_\lambda\mathcal{H}|n\rangle}{E_n - E_m}. \tag{70}$$

Using this result we can rewrite the components of the geometric tensor as

$$\chi_{\alpha\beta} = \sum_{n\neq 0}\langle 0|\overleftarrow{\partial}_\alpha|n\rangle\langle n|\partial_\beta|0\rangle = -\sum_{n\neq 0}\langle 0|\partial_\alpha|n\rangle\langle n|\partial_\beta|0\rangle = \sum_{n\neq 0}\frac{\langle 0|\partial_\alpha\mathcal{H}|n\rangle\langle n|\partial_\beta\mathcal{H}|0\rangle}{(E_n - E_0)^2} \tag{71}$$

Now let us use the following trick standard in connecting the Lehmann's representation of some observable to the non-equal time correlation functions:

$$\frac{1}{(E_n - E_0)^2} = \int_0^\infty d\omega\frac{1}{\omega^2}\delta(E_n - E_0 - \omega) = \int_0^\infty d\omega\int_{-\infty}^\infty\frac{dt}{2\pi}\mathrm{e}^{-i(E_n - E_0 - \omega)t}. \tag{72}$$

In this integral we can always add $\exp[-\epsilon|t|]$ for the convergence. Next we note that

$$\langle 0|\mathrm{e}^{iE_0 t}\partial_\alpha\mathcal{H}\mathrm{e}^{-iE_n t}|n\rangle = \langle 0|\partial_\alpha\mathcal{H}(t)|n\rangle \tag{73}$$

is the matrix element of the operator $\partial_\alpha\mathcal{H}$ in the Heisenberg representation. Plugging this into Eq. (71) we find

$$\chi_{\alpha\beta} = \int_0^\infty \frac{d\omega}{\omega^2} S_{\alpha\beta}(\omega), \tag{74}$$

where

$$S_{\alpha\beta}(\omega) = \int_{-\infty}^{\infty} \frac{dt}{2\pi}\mathrm{e}^{i\omega t}\langle 0|\partial_\alpha\mathcal{H}(t)\partial_\beta\mathcal{H}(0)|0\rangle_c. \tag{75}$$

This object $S_{\alpha\beta}(\omega)$ is a standard response coefficient. Its symmetric part, determining the metric tensor, appears in the noise, full counting statistics and the absorption spectrum (through the fluctuation-dissipation relations). Its antisymmetric part determining the Berry curvature appears in the standard Kubo linear response. This implies that both the metric tensor and the Berry curvature are measurable quantities in standard experimental setups.

III. GEOMETRIC INVARIANTS: GEOMETRY OF THE XY CHAIN.

Both the Berry curvature and the Fubini-Study metric tensor define geometric (topological) invariants. There are many of those. In these lecture notes we will concentrate on two most important ones: (first) Chern number and the Euler characteristic. Because the Chern number has been extensively discussed in literature in many different contexts we will mention it only briefly and will concentrate on the Euler characteristic, which has been discussed much less with respect to physical systems. Also in this section we will focus exclusively on two-dimensional manifolds. Geometry and topology of higher-dimensional manifolds is much more complex and is often understood through various two-dimensional cuts in any case.

A. Basic definitions of the Euler characteristic and the first Chern number.

The Euler characteristic of the metric manifold $\mathcal{M}$ is an integer equal to the integrated Gauss curvature over the manifold with an additional boundary term:

$$\xi(\mathcal{M}) = \frac{1}{2\pi}\left[\int_{\mathcal{M}} K dS + \oint_{\partial\mathcal{M}} k_g dl\right], \tag{76}$$

A standard notation for the Euler characteristic is χ but because we reserved this symbol for the geometric tensor we will use ξ instead. The two terms on the left side of Eq. (76) are the bulk and boundary contributions to the Euler characteristic of the manifold. We refer to the first term,

$$\xi_{\text{bulk}}(\mathcal{M}) = \frac{1}{2\pi}\int_{\mathcal{M}} K dS \ , \tag{77}$$

and the second term,

$$\xi_{\text{boundary}}(\mathcal{M}) = \frac{1}{2\pi}\oint_{\partial\mathcal{M}} k_g dl \ , \tag{78}$$

as the bulk and boundary Euler integrals, respectively. These terms, along with their constituents – the Gaussian curvature (K), the geodesic curvature (k_g), the area element (dS), and the line element (dl) – are *geometric invariants*, meaning that they remain unmodified under any change of variables. More explicitly, if the metric is written in first fundamental form as

$$ds^2 = E d\lambda_1^2 + 2F d\lambda_1 d\lambda_2 + G d\lambda_2^2 \ , \tag{79}$$

then these invariants are given by (Kreyszig, 1959)

$$\begin{aligned} K &= \frac{1}{\sqrt{g}}\left[\frac{\partial}{\partial\lambda_2}\left(\frac{\sqrt{g}\,\Gamma_{11}^2}{E}\right) - \frac{\partial}{\partial\lambda_1}\left(\frac{\sqrt{g}\,\Gamma_{12}^2}{E}\right)\right] \\ k_g &= \sqrt{g}G^{-3/2}\Gamma_{22}^1 \\ dS &= \sqrt{g}d\lambda_1 d\lambda_2 \\ dl &= \sqrt{G}d\lambda_2 \ , \end{aligned} \tag{80}$$

where k_g and dl are given for a curve of constant λ_1. The metric determinant g and Christoffel symbols Γ_{ij}^k are

$$g = EG - F^2 \tag{81}$$

$$\Gamma_{ij}^k = \frac{1}{2}g^{km}\left(\partial_j g_{im} + \partial_i g_{jm} - \partial_m g_{ij}\right) \ , \tag{82}$$

where g^{ij} is the inverse of the metric tensor g_{ij}. As we see the explicit expressions for the Euler characteristic are quite cumbersome but they are known and unique functions of the metric tensor. A simple intuitive understanding of the Gauss curvature in two dimensions comes from

$$K = \frac{1}{R_1 R_2},$$

where R_1 and R_2 are the principal radii of curvature., which are the minimal and the maximal radii of the circles touching the surface. The geodesic curvature is a curvature of the boundary

projected to the tangent plane. Thus e.g. for a sphere the geodesic curvature of a great circle is zero. In simple words the geodesic curvature measures the distance of the boundary from the geodesic. For the manifolds without boundaries like a torus or a sphere the Euler characteristic simply counts the number of holes in the manifold. Thus for a sphere the Euler characteristic is $\xi = 2$ for a torus $\xi = 0$ and each additional hole gives an extra contribution of -2.

The other important topological characteristic is the (first) Chern number, which is defined through the Berry curvature. To understand where it comes from let us consider a closed manifold like shown in Fig. 1 and choose an arbitrary closed contour on that sphere like a dashed line. Let us compute the Berry phase (flux) along this contour by two ways:

$$\gamma_{top} = \int_{S_{top}} F_{\alpha\beta} d\lambda_\alpha d\lambda_\beta, \quad \gamma_{bottom} = -\int_{S_{bottom}} F_{\alpha\beta} d\lambda_\alpha d\lambda_\beta, \tag{83}$$

where the minus sign in the second term appears because the top and bottom surfaces of the sphere bounded by the curve have opposite orientations with respect to this curve, which can be checked by e.g. thumb rule. Recall that γ represents the physical phase acquired by the wave function during the (adiabatic) motion in the parameter space. Since the wave function is unique the two phases should be identical up to an overall constant $2\pi n$. Thus we find that

$$2\pi n = \gamma_{top} - \gamma_{bottom} = \oint_S F_{\alpha\beta} d\lambda_\alpha d\lambda_\beta \tag{84}$$

The integer n is precisely the Chern number ch_1 so we get

$$\mathrm{ch}_1 = \frac{1}{2\pi} \oint_S F_{\alpha\beta} d\lambda_\alpha \wedge d\lambda_\beta \tag{85}$$

As we found earlier for a spin one half particle in a magnetic field $F_{\theta\phi} = 1/2 \sin(\theta)$ so in this case

$$\mathrm{ch}_1 = \frac{1}{2\pi} \int_0^{2\pi} d\phi \int_0^{\pi} d\theta \frac{1}{2} \sin(\theta) = 1 \tag{86}$$

One can easily check that for a particle with a spin S this Chern number is equal to $2S$.

Exercise

- Prove the statement above.

B. Geometric structure of the XY chain.

Let us now analyze geometric invariants for a particular XY chain model. This model is sufficiently simple so that all calculations can be done explicitly analytically but yet it has a very rich

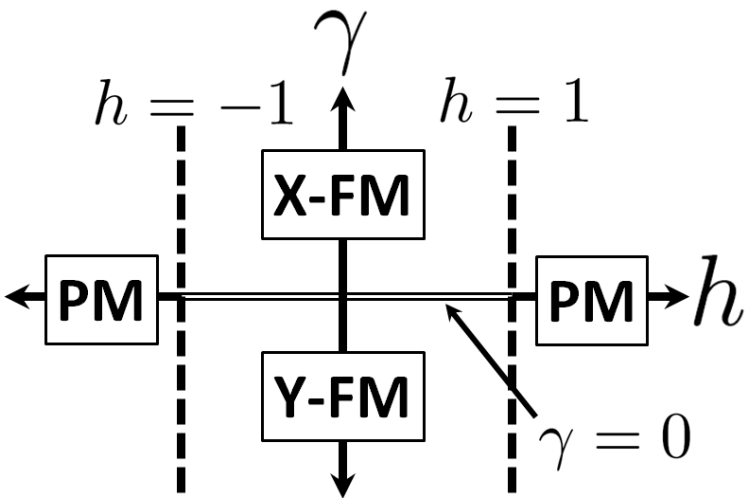

FIG. 2 Ground state phase diagram of the XY Hamiltonian (Eq. (89)) for $\phi = 0$. The rotation parameter ϕ modifies the Ising ferromagnetic directions, otherwise maintaining all features of the phase diagram. As a function of transverse field h and anisotropy γ, the ground state undergoes continuous Ising-like phase transitions between paramagnet and ferromagnet at $h = \pm 1$ and anisotropic transitions between ferromagnets aligned along X and Y directions (X/Y-FM) at $\gamma = 0$. These two types of phase transition meet at multi-critical points.

phase diagram with two different phase transitions and multicritical points. The content of this chapter is adopted from Ref. (Kolodrubetz *et al.*, 2013).

Quantum XY chain described by the Hamiltonian

$$\mathcal{H} = -\sum_j \left[J_x \sigma_j^x \sigma_{j+1}^x + J_y \sigma_j^y \sigma_{j+1}^y + h\sigma_j^z \right] , \tag{87}$$

where $J_{x,y}$ are exchange couplings, h is a transverse field, and the spins are represented as Pauli matrices $\sigma^{x,y,z}$. It is convenient to re-parameterize the model in terms of new couplings J and γ as

$$J_x = J\left(\frac{1+\gamma}{2}\right),\ J_y = J\left(\frac{1-\gamma}{2}\right) , \tag{88}$$

where J is the energy scale of the exchange interaction and γ is its anisotropy. We add an additional tuning parameter ϕ, corresponding to simultaneous rotation of all the spins about the z-axis by angle $\phi/2$. While rotating the angle ϕ has no effect on the spectrum of $\mathcal{H}$, it does modify the ground state wave function. To fix the overall energy scale, we set $J = 1$.

The Hamiltonian described above can be written as

$$\mathcal{H}(h,\gamma,\phi) = -\sum_j \left[\sigma_j^+ \sigma_{j+1}^- + \text{h.c.}\right] - \gamma \sum_j \left[e^{i\phi}\sigma_j^+ \sigma_{j+1}^+ + \text{h.c.}\right] - h\sum_j \sigma_j^z . \tag{89}$$

Since the Hamiltonian is invariant under the mapping $\gamma \to -\gamma$, $\phi \to \phi + \pi$, we generally restrict ourselves to $\gamma \geq 0$. This model has a rich phase diagram (Damle and Sachdev, 1996), as shown in Fig. 2. There is a phase transition between paramagnet and Ising ferromagnet at $|h| = 1$ and $\gamma \neq 0$. There is an additional critical line at the isotropic point ($\gamma = 0$) for $|h| < 1$. The two transitions meet at multi-critical points when $\gamma = 0$ and $|h| = 1$. Another notable line is $\gamma = 1$, which corresponds to the transverse-field Ising (TFI) chain. Finally let us note that there are two other special lines $\gamma = 0$ and $|h| > 1$ where the ground state is fully polarized along the magnetic field and thus h-independent. These lines are characterized by vanishing susceptibilities including vanishing metric along the h-direction. One can show that such state is fully protected by the rotational symmetry of the model and can be terminated only at the critical (gapless) point (Kolodrubetz *et al.*, 2013). The phase diagram is invariant under changes of the rotation angle ϕ.

Rewriting the spin Hamiltonian in terms of free fermions via a Jordan-Wigner transformation, $\mathcal{H}$ can be mapped to an effective non-interacting spin one-half model(Sachdev, 1999) with

$$\mathcal{H} = \sum_k \mathcal{H}_k; \quad \mathcal{H}_k = -\begin{pmatrix} h - \cos(k) & \gamma \sin(k) \mathrm{e}^{i\phi} \\ \gamma \sin(k) \mathrm{e}^{-i\phi} & -[h - \cos(k)] \end{pmatrix}.$$

The ground state of $\mathcal{H}_k$ is a Bloch vector with azimuthal angle ϕ and polar angle

$$\theta_k = \tan^{-1}\left[\frac{\gamma \sin(k)}{h - \cos(k)}\right]. \tag{90}$$

Because the Hamiltonian effectively describes an independent set of two-level systems we can immediately extend the results from the previous section to find the expression for different metric tensor components.

In particular differentiating the ground state in each momentum sector with respect to h we find

$$\partial_h |\mathrm{gs}_k\rangle = \frac{\partial_h \theta_k}{2} \begin{pmatrix} -\sin\left(\frac{\theta_k}{2}\right) e^{i\phi/2} \\ \cos\left(\frac{\theta_k}{2}\right) e^{-i\phi/2} \end{pmatrix} = -\frac{\partial_h \theta_k}{2} |\mathrm{es}_k\rangle. \tag{91}$$

The same derivation applies to the anisotropy γ, since changing either γ or h only modifies θ_k and not ϕ. Thus we find

$$\mathcal{A}_\lambda = \frac{1}{2} \sum_k \left(\partial_\lambda \theta_k\right) \tau_k^y, \tag{92}$$

where $\lambda = \{h, \gamma\}$ and $\tau_k^{x,y,z}$ are Pauli matrices that act in the instantaneous ground/excited state basis. Similarly, for the parameter ϕ, we find that

$$\mathcal{A}_\phi = -\frac{1}{2} \sum_k \left[\cos(\theta_k)\tau_k^z + \sin(\theta_k)\tau_k^x\right]. \tag{93}$$

Using that

$$g_{\mu\nu} = \frac{1}{2}\langle gs|\mathcal{A}_\mu\mathcal{A}_\nu + \mathcal{A}_\nu\mathcal{A}_\mu|gs\rangle \tag{94}$$

we find

$$g_{hh} = \frac{1}{4}\sum_k \left(\frac{\partial\theta_k}{\partial h}\right)^2,\ g_{\gamma\gamma} = \frac{1}{4}\sum_k \left(\frac{\partial\theta_k}{\partial\gamma}\right)^2,\ g_{h\gamma} = \frac{1}{4}\sum_k \frac{\partial\theta_k}{\partial h}\frac{\partial\theta_k}{\partial\gamma},\ g_{\phi\phi} = \frac{1}{4}\sum_k \sin^2(\theta_k), \tag{95}$$

The remaining two components of the metric tensor $g_{h\phi}$, $g_{\gamma\phi}$ are equal to zero.

The expressions for the metric tensor can be evaluated in the thermodynamic limit, where the summation becomes integration over momentum space. It is convenient to divide all components of the metric tensor by the system size and deal with intensive quantities $g_{\mu\nu} \to g_{\mu\nu}/L$. Then one calculates these integrals to find that

$$\begin{aligned}
g_{\phi\phi} &= \frac{1}{8}\begin{cases} \frac{|\gamma|}{|\gamma|+1}, & |h|<1 \\ \frac{\gamma^2}{1-\gamma^2}\left(\frac{|h|}{\sqrt{h^2-1+\gamma^2}}-1\right), & |h|>1 \end{cases} \\
g_{hh} &= \frac{1}{16}\begin{cases} \frac{1}{|\gamma|(1-h^2)}, & |h|<1 \\ \frac{|h|\gamma^2}{(h^2-1)(h^2-1+\gamma^2)^{3/2}}, & |h|>1 \end{cases} \\
g_{\gamma\gamma} &= \frac{1}{16}\begin{cases} \frac{1}{|\gamma|(1+|\gamma|)^2}, & |h|<1 \\ \left(\begin{array}{c} \frac{2}{(1-\gamma^2)^2}\left[\frac{|h|}{\sqrt{h^2-1+\gamma^2}}-1\right]- \\ \frac{|h|\gamma^2}{(1-\gamma^2)(h^2-1+\gamma^2)^{3/2}} \end{array}\right), & |h|>1 \end{cases} \\
g_{h\gamma} &= \frac{1}{16}\begin{cases} 0, & |h|<1 \\ \frac{-|h|\gamma}{h(h^2-1+\gamma^2)^{3/2}}, & |h|>1 \end{cases}
\end{aligned} \tag{96}$$

Using the metric tensor we can visualize the ground state manifold by building an equivalent (i.e., isometric) surface and plotting its shape. It is convenient to focus on a two-dimensional manifold by fixing one of the parameters. We then represent the two-dimensional manifold as an equivalent three-dimensional surface. To start, let's fix the anisotropy parameter γ and consider the $h-\phi$ manifold. Since the metric tensor has cylindrical symmetry, so does the equivalent surface. Parameterizing our shape in cylindrical coordinates and requiring that

$$dz^2 + dr^2 + r^2 d\phi^2 = g_{hh}dh^2 + g_{\phi\phi}d\phi^2\ , \tag{97}$$

we see that

$$r(h) = \sqrt{g_{\phi\phi}},\ z(h) = \int_0^h dh_1 \sqrt{g_{hh}(h_1) - \left(\frac{dr(h_1)}{dh_1}\right)^2}. \tag{98}$$

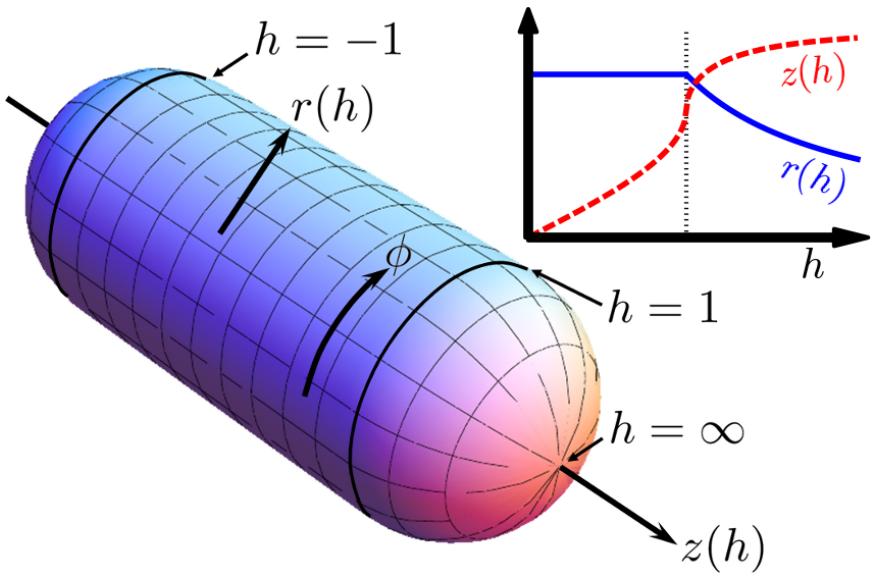

FIG. 3 Equivalent graphical representation of the phase diagram of the transverse field Ising model ($\gamma = 1$) in the $h - \phi$ plane. The ordered ferromagnetic phase maps to a cylinder of constant radius. The disordered paramagnetic phases $h > 1$ and $h < -1$ map to the two hemispherical caps. The inset shows how the cylindrical coordinates z and r depend on the transverse field h.

Using Eq. (96), we explicitly find the shape representing the XY chain. In the Ising limit ($\gamma = 1$), we get

$$\begin{cases} r(h) = \frac{1}{4} \\ z(h) = \frac{\arcsin(h)}{4} \end{cases} \quad |h| < 1,$$
$$\begin{cases} r(h) = \frac{1}{4|h|} \\ z(h) = \frac{\pi}{8}\frac{|h|}{h} + \frac{\sqrt{h^2-1}}{4h} \end{cases} \quad |h| > 1\ . \tag{99}$$

The phase diagram is thus represented by a cylinder of radius 1/4 corresponding to the ferromagnetic phase capped by the two hemispheres representing the paramagnetic phase, as shown in Fig. 3. It is easy to check that the shape of each phase does not depend on the anisotropy parameter γ, which simply changes the aspect ratio and radius of the cylinder. Because of the relation $r(h) = \sqrt{g_{\phi\phi}}$ this radius vanishes as the anisotropy parameter γ goes to zero. By an elementary integration of the Gaussian curvature, the phases have bulk Euler integral 0 for the ferromagnetic cylinder and 1 for each paramagnetic hemisphere. These numbers add up to 2 as required, since the full phase diagram is homeomorphic to a sphere. From Fig. 3, it is also clear that the phase boundaries at $h = \pm 1$ are geodesics, meaning that the geodesic curvature (and thus the boundary contribution ξ_{boundary}) is zero for a contour along the phase boundary. This boundary integral protects the value of the bulk integral and vice versa.

In the Ising limit ($\gamma = 1$), the shape shown in Fig. 3, can also be easily seen from computing the curvature K using Eq. (80). Within the ferromagnetic phase, the curvature is zero – no surprise, given that the metric is flat by inspection. The only shape with zero curvature and cylindrical symmetry is a cylinder. Similarly, within the paramagnet, the curvature is a constant $K = 16$, like that of a sphere. Therefore, to get cylindrical symmetry, the phase diagram is clearly seen to be a cylinder capped by two hemispheres.

We can also reconstruct an equivalent shape in the $\gamma - \phi$ plane. In this case we expect to see a qualitative difference for $|h| > 1$ and $|h| < 1$ because in the latter case there is an anisotropic phase transition at the isotropic point $\gamma = 0$, while in the former case there is none. These two shapes are shown in Fig. 4. The anisotropic phase transition is manifest in the conical singularity developing at $\gamma = 0$.[4]

The singularity at $\gamma = 0$ yields a non-trivial bulk Euler integral for the anisotropic phase transition. To see this, consider the bulk integral

$$\xi_{\text{bulk}}(\epsilon) = \lim_{L\to\infty} \int_0^{2\pi} d\phi \int_\epsilon^\infty d\gamma \, \sqrt{g(\gamma,\phi)} K(\gamma,\phi) \ . \tag{100}$$

In the limit $\epsilon \to 0^+$, this integral has a discontinuity as a function of h at the phase transition, as seen in Fig. 4. Thus, $\xi_{\text{bulk}} \equiv \xi_{\text{bulk}}(\epsilon = 0^+)$ can be used as a geometric characteristic of the anisotropic phase transition. Direct calculation shows that $\xi_{\text{bulk}} = 1/\sqrt{2}$ in the ferromagnetic phase and $\xi_{\text{bulk}} = 1$ in the paramagnetic phase. This non-integer geometric invariant is due to the existence of a conical singularity.

A careful analysis shows that in both cases the bulk Euler characteristics are protected by the universality of the transition. I.e. if one adds extra terms to the Hamiltonian, which do not qualitatively affect the phase diagram the bulk Euler characteristic does not change. The details of the proof are available in Ref. (Kolodrubetz *et al.*, 2013). But the basic idea is very simple. The sum of the bulk and the boundary Euler characteristics is protected by the geometry of the parameter manifold. As long as the boundary of the manifold coincides with the phase boundary all components of the metric tensor become universal (Campos Venuti and Zanardi, 2007). Therefore it is not surprising that the geodesic curvature also becomes universal and thus the boundary Euler characteristic is protected. As a result the bulk Euler characteristic is protected too. It is interesting that unlike critical exponents the bulk Euler characteristic truly characterizes

[4] We note a potential point of confusion, namely that a naive application of Eq. (80) would seem to indicate that the curvature is a constant $K = 4$ in the ferromagnetic phase for $\gamma > 0$, in which case the singularity at $\gamma = 0$ is not apparent. However, a more careful derivation shows that the curvature is indeed singular at $\gamma = 0$: $K = 4 - 8(1-\gamma)\frac{\partial^2}{\partial^2\gamma}|\gamma| = 4 - 16\delta(\gamma)$, where $\delta(\gamma)$ is the Dirac delta function.

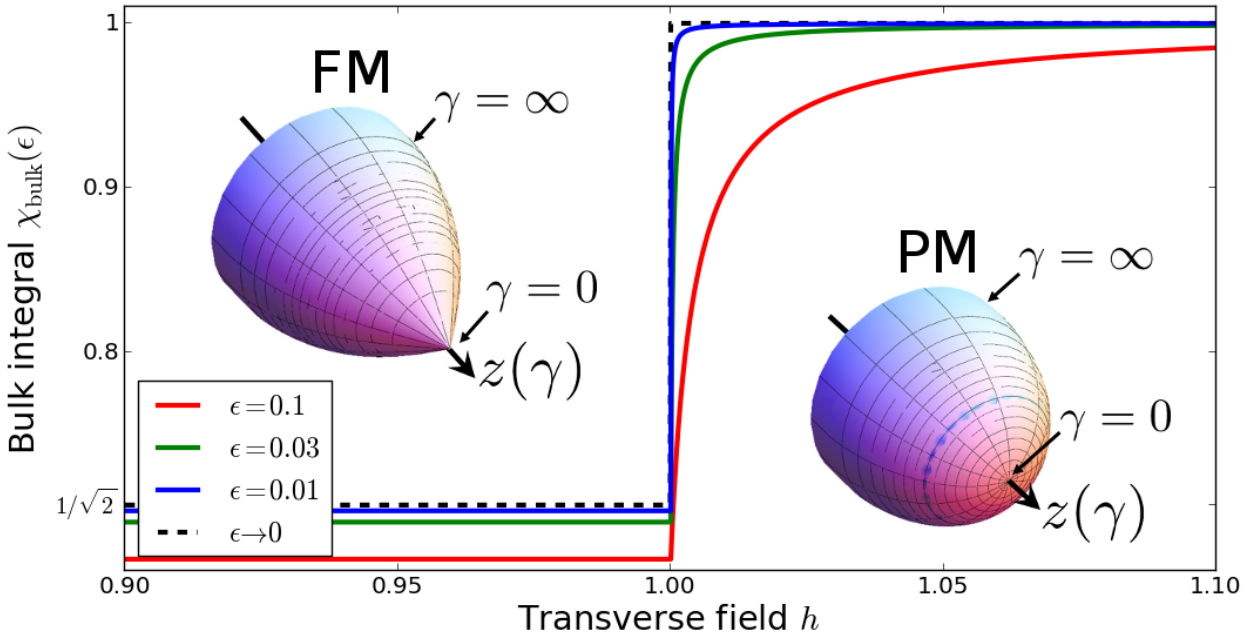

FIG. 4 (insets) Equivalent graphical representation of the phase diagram of the XY model in the $\gamma - \phi$ plane, where $\gamma \in [0, \infty)$ and $\phi \in [0, 2\pi]$. The right inset shows the paramagnetic disordered phase and the left inset represents the ferromagnetic phase. It is clear that in the latter case there is a conical singularity developing at $\gamma = 0$ which represents the anisotropic phase transition. The plots show bulk Euler integral $\xi_{\text{bulk}}(\epsilon)$, demonstrating the jump in ξ_{bulk} at the phase transition between the paramagnet and ferromagnet in the limit $\epsilon \to 0^+$.

the phase transition and does not depend on the parametrization. One can also analyze the Euler characteristic and the Gauss curvature of the in the $h-\gamma$ plane. One finds additional nonintegrable curvature singularities near the anisotropic phase transition and near the multi-critical point.

IV. GAUGE POTENTIALS AND NON-ADIABATIC RESPONSE

A. Dynamical Quantum Hall effect

We already noted in the first section that the gauge potentials appear in the Galilean term in the moving Hamiltonian:

$$\mathcal{H}_m = U^\dagger \mathcal{H} U - \dot{\lambda}_\alpha \mathcal{A}_\alpha = \tilde{\mathcal{H}} - \dot{\lambda}_\alpha \mathcal{A}_\alpha. \tag{101}$$

The Hamiltonian $\tilde{\mathcal{H}}$ is diagonal and thus only produces shifts in the energies but does not couple them (i.e. does not have any off-diagonal matrix elements) so it is not responsible for the transitions between levels. Conversely the Galilean term is in general off-diagonal and thus causes the transitions between levels. Near the adiabatic limit the Galilean term is small and thus can be

treated as a perturbation.

Let us first consider the setup where the system is initially prepared at equilibrium (for concreteness in the ground state) at some initial value of the coupling $\vec{\lambda}_0 \equiv \vec{\lambda}(t=0)$. Then the coupling starts changing in time. To avoid need of worrying about initial transients, which can be done but makes derivations more involved, we will assume that the rate of change of the coupling is a smooth function of time. Under this smooth transformation in the leading order in $|\dot{\lambda}|$ the system follows the ground state of the moving Hamiltonian $\mathcal{H}_m$. One can worry whether the adiabatic theorem applies to this Hamiltonian, which is still time-dependent. Later we will give a rigorous derivation of the result (alternatively see Ref. (Gritsev and Polkovnikov, 2012) for more details). Loosely speaking the Galilean term removes the leading non-adiabatic contribution from the Hamiltonian. The higher order corrections will be of the higher order in $|\dot{\lambda}|^2$. When we do the measurement of any observable in the system like magnetization, on the other hand, we typically do it in the lab frame. Recall that we introduced the moving frame just for convenience. One can thus view the instantaneous measurement process as sudden quench, where the rate $\dot{\lambda}$ is quenched to zero.

Within the first order of perturbation theory the transition amplitudes to the excited states due to such quench are given by

$$a_n = -\dot{\lambda}_\alpha \frac{\langle n|\mathcal{A}_\alpha|0\rangle}{E_n - E_0} \tag{102}$$

Next we compute the leading order correction to the observables due to this quench. It is convenient to represent observables as generalized forces conjugate to some other coupling λ_β:

$$\mathcal{M}_\beta = -\partial_\beta \mathcal{H}. \tag{103}$$

The matrix elements of these objects already appeared in the definition of the geometric tensor so it is convenient to continue dealing with them. Note that any observable can be represented as some generalized force. E.g. the magnetization is conjugate to the magnetic field, current is conjugate to a vector potential, nearest neighbor correlation function is conjugate to the nearest neighbor hopping or interaction etc. Then we find that

$$M_\beta \equiv \langle\psi|\mathcal{M}_\beta|\psi\rangle \approx M_\beta^{(0)} - \dot{\lambda}_\alpha \sum_{n\neq 0} (a_n^* \langle n|\partial_\beta \mathcal{H}|0\rangle + a_n \langle 0|\partial_\beta \mathcal{H}|n\rangle = M_\beta^{(0)} + i\dot{\lambda}_\alpha \sum_{n\neq 0} \frac{\langle 0|\partial_\alpha|n\rangle\langle n|\partial_\beta \mathcal{H}|0\rangle - \langle 0|\partial_\beta \mathcal{H}|n\rangle\langle n|\partial_\alpha|0\rangle}{E_n - E_0} = M_\beta^{(0)} + F_{\beta\alpha}\dot{\lambda}_\alpha, \tag{104}$$

where $M_\beta^{(0)}$ is the generalized force evaluated in the instantaneous ground state. The last equality immediately follows from Eq. (70). The equation above constitutes the dynamical Quantum Hall

effect. It shows that the leading non-adiabatic (Kubo) correction to the generalized force comes from the product of the Berry curvature and the rate of change of the parameter $\vec{\lambda}$.

Let us illustrate that this relation reduces to the standard integer quantum Hall effect (QHE). We will make only two generic assumptions: (i) the ground state of the system is not-degenerate (degeneracies can lead to the fractional QHE) and (ii) the Hamiltonian of the system can be represented in the form

$$\mathcal{H} = \sum_{j=1}^{N} \frac{\left(\vec{p}_j - \frac{e}{c}\vec{\Lambda}_j\right)^2}{2m_j} + V(\vec{r}_1, \vec{r}_2, \dots \vec{r}_N), \tag{105}$$

where V is an arbitrary momentum independent potential which can include both interactions between particles and the external potential. We remind that we use the $\vec{\Lambda}_j \equiv \vec{\Lambda}(\vec{q}_j)$ notation for the vector potential to avoid the confusion with the gauge potential. Let us assume that the vector potential consists of some static part (not necessarily uniform) representing a static magnetic field and an extra dynamic part representing the electric field in the system (recall that in the Coulomb gauge $\vec{\mathcal{E}} = 1/c\,\partial_t\vec{\Lambda}$). We will choose the components of the time-dependent vector potential divided by speed of light as our parameters (or coordinates), i.e.

$$\lambda_x = \frac{1}{c}\Lambda_x,\ \lambda_y = \frac{1}{c}\Lambda_y. \tag{106}$$

Note that the generalized force with respect to λ_y is

$$\mathcal{M}_y = -\partial_{\lambda_y}\mathcal{H} = \sum_j \frac{e}{m_j}\left(p_j^{(y)} - \frac{e}{c}\Lambda_j^{(y)}\right) = \mathcal{J}_y, \tag{107}$$

which is the current operator along the y-direction. Clearly in the absence of the electric field there is no current so the dynamical Hall relation reads

$$J_y = \hbar F_{\lambda_y,\lambda_x}\mathcal{E}_x, \tag{108}$$

where we explicitly included the factor of $\hbar$ omitted in Eq. (104). This factor must be there to fix the dimensions, or alternatively can be obtained by noting that the gauge potentials are actually $\mathcal{A}_\alpha = i\hbar\partial_\alpha$. To find the Hall conductivity we note that the total current is related to the two-dimensional current density via

$$J_y = L_x L_y j_y, \tag{109}$$

where L_x and L_y are the dimensions of the sample. Therefore the Hall conductivity $\sigma_{yx} = j_y/\mathcal{E}_x$ is related to the Berry curvature via

$$\sigma_{xy} = \frac{\hbar F_{\lambda_x\lambda_y}}{L_x L_y}. \tag{110}$$

Now let us use the fact that the Chern number related to the integral of the Berry curvature over the closed manifold is an integer. Because of the assumed form of the Hamiltonian the uniform and thus curl-free vector potential (which leads to the uniform electric field) can be gauged away by absorbing it into the phase of the wave function like in the Aharonov-Bohm geometry. Thus the acquired phase by the wave-function is

$$\phi = \frac{e}{c\hbar}\int(\Lambda_x dx + \Lambda_y dy) = \frac{e}{\hbar}(\lambda_x L_x + \lambda_y L_y) \tag{111}$$

Clearly this phase acquires the winding of 2π if λ_x changes between 0 and $2\pi\hbar/(eL_x)$ and similarly for λ_y. So the parameter manifold is effectively a torus of the area $4\pi^2\hbar^2/(e^2L_xL_y)$. Because the Berry curvature is independent of the vector potential (since it only affects the overall phase of the wave function) the Chern number is just the product of the Berry curvature and the area divided by 2π:

$$\mathrm{ch}_1 = \frac{1}{2\pi}F_{\lambda_x\lambda_y}\frac{4\pi^2\hbar^2}{e^2L_xL_y} \tag{112}$$

or equivalently

$$F_{\lambda_x\lambda_y} = \frac{e^2L_xL_y}{2\pi\hbar^2}\mathrm{ch}_1. \tag{113}$$

Combining this with the expression for the Hall conductivity we find

$$\sigma_{xy} = \frac{\hbar}{L_xL_y}\frac{e^2L_xL_y}{2\pi\hbar^2}\mathrm{ch}_1 = \frac{e^2}{2\pi\hbar}\mathrm{ch}_1, \tag{114}$$

which precisely constitutes the integer quantum Hall effect. This simple derivation highlights that the quantum Hall effect can be thought of as the linear non-adiabatic response of the system to the time-dependent vector potential. Note that this derivation does not require assuming any particular boundary conditions. We relied on the periodicity of the wave function in the vector-potential space not in real space.

The second example we discuss is a again a spin in a time-dependent magnetic field. Namely we will assume that the parameters θ and ϕ characterizing the angles of the external magnetic field change in time. Suppose that the spin is prepared in the ground state along the magnetic field and then the latter starts changing in time e.g. along the θ-direction. The generalized force along the orthogonal ϕ-direction is just the ϕ-component of the magnetization. In the adiabatic limit it is clearly zero since in this case the magnetization simply follows the magnetic field. The leading non-adiabatic correction is then given by the Berry curvature:

$$m_\phi \approx F_{\phi\theta}\dot{\theta}. \tag{115}$$

Likewise

$$m_\theta \approx F_{\theta\phi}\dot{\phi}. \tag{116}$$

in experiments it is easier to measure the magnetization along the y-direction. Then if the magnetic field has a time dependent x-component and a time independent z-component we have

$$m_y = F_{yx}\dot{h}_x, \tag{117}$$

where

$$F_{yx} = \frac{1}{2h^2}\cos(\theta). \tag{118}$$

From this expression it is easy to recover $F_{\theta\phi}$ by a standard transformation to the spherical coordinates:

$$F_{\theta\phi} = h^2 F_{yx}\tan(\theta) = \frac{1}{2}\sin(\theta). \tag{119}$$

In Fig. 5 we show numerically computed dependence of the transverse y-magnetization on the rate of change of the magnetic field v for a particular protocol

$$\mathcal{H} = -\sigma_z - h_x(t)\sigma_x, \tag{120}$$

where $h_x(t) = 0.5 + vt$. The transverse magnetization is computed at time $t = 0$ and the initial condition corresponds to the ground state at large negative time $t = -100/v$. As it is evident from the figure at slow rates dependence of the transverse magnetization on the rate is linear and the slope is exactly given by the Berry curvature. Integrating the Berry curvature over the angles of the field one can measure the Chern number.

It is interesting that even within such a simple system one can already observe the topological phase transition where the Chern number changes from 0 to 1. For this we can consider a slight modification into the Hamiltonian by adding a constant static magnetic field along the z direction.

$$\mathcal{H} = -\frac{1}{2}\left[h_0\sigma_z + h_1\cos(\theta)\sigma^z + h_1\sin(\theta)\cos(\phi)\sigma^x + h_1\sin(\theta)\sin(\phi)\sigma^y\right]. \tag{121}$$

Then as one changes the magnetic field h_1 along the sphere of constant radius at fixed h_0 we can have two different scenarios. First when $h_0 < h_1$ corresponds to the total magnetic field encircling the origin $h = 0$ and thus producing the Chern number equal to one. The second scenario is realized when $h_0 > h_1$. Then the total magnetic field does not enclose the origin and the Chern number is zero. The easiest way to see this is to take the limit $h_1 \to 0$ and recall that the Chern

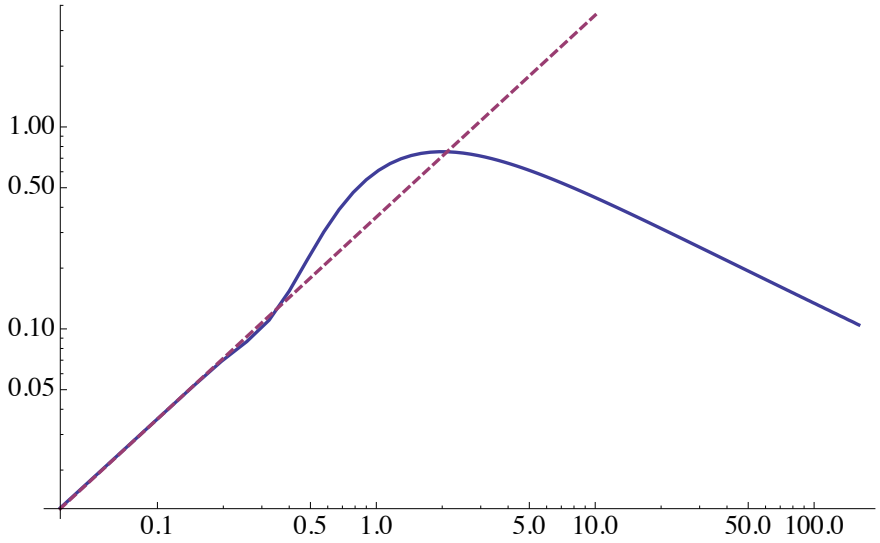

FIG. 5 Dependence of the transverse magnetization on the rate of change of the magnetic field along the x-direction (see text for details

number can not change unless the surface crosses a gapless crossing point. This phase transition was recently observed in experiments on superconducting qubits (M. Schroer et. al., unpublished). Recall that the Chern number is the total flux of the Berry curvature (magnetic field) and it only depends on whether the gapless crossing point $h = 0$ is enclosed by the integration surface or not. This situation is very similar to the electrostatics, where the electric field flux through a closed surface only depends on the total charge inside this surface. Thus the level crossing point plays the role of the magnetic monopole (similarly to the unit electric charge being the electric monopole). Monopoles appear in more complicated systems and can not simply disappear under small perturbations (because the Chern number is protected in any gapped phase). Thus contrary to the common wisdom the level crossing points are protected and if one introduces some generic perturbation they just move around in the parameter space.

This simple topological transition is actually equivalent to the transition from the normal to the topological insulator realized e.g. in the Haldane model (Haldane, 1988). We will not go into the details of this model, we only point that the model represents a single particle band of a two dimensional honeycomb lattice which has two sublattices and a particular form of hoppings. At each Bloch momentum $\vec{k}$ the Hamiltonian is effectively described by the 2×2 matrix, which is equivalent to the spin one half system in a $\vec{k}$-dependent magnetic field. One defines the Chern number of the band as

$$\frac{1}{2\pi} \int \int dk_x \, dk_y F_{k_x,k_y}, \tag{122}$$

where

$$F_{k_x,k_y} = i(\langle \partial_{k_x}\psi | \partial_{k_y}\psi \rangle - \langle \partial_{k_y}\psi | \partial_{k_x}\psi \rangle).$$

Because the Brillouin zone is a closed manifold (equivalent to a torus) this band Chern number is either zero or one depending on the parameters of the Hamiltonian. The transition between the bands with different Chern numbers is called topological phase transition. In Fig. 6 we pictorially

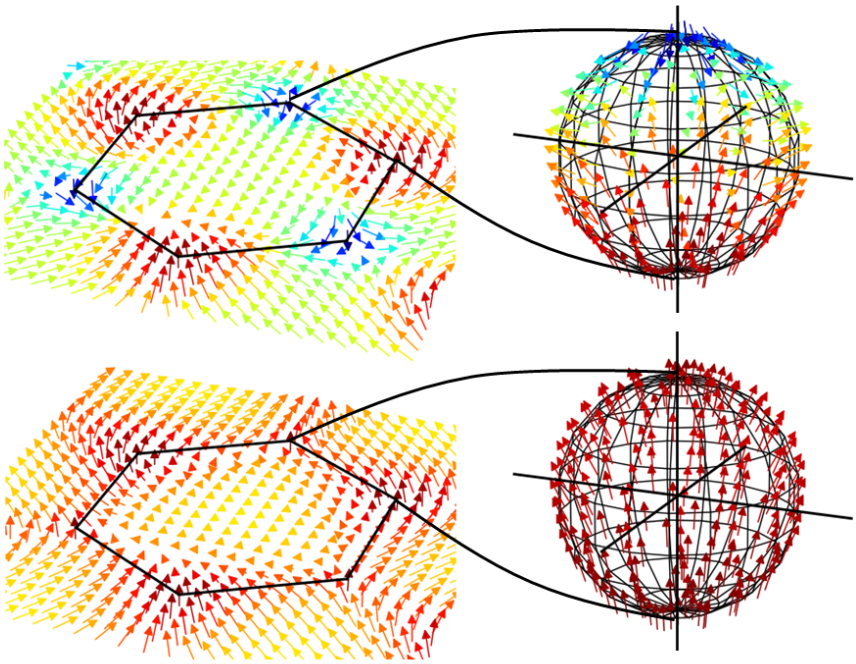

FIG. 6 Schematic representation of the mapping of the effective magnetic field in the Haldane model to the spin one half system. In the topologically nontrivial phase the magnetic field wraps around the sphere. Plot is courtesy of M. Kolodrubetz.

show how the mapping of the Haldane model to a spin one half particle in a magnetic field works. In the topologically non-trivial phase the effective magnetic field wraps around the sphere, which in our language corresponds to $h_1 > h_0$ and vice versa. It is interesting that we were able to define the topological phase transition for just one spin. This works because we consider not one ground state but rather the whole manifold of ground states, which maps to a completely filled band of an insulator.

We used a simple single-particle problem as an illustration. The situation becomes much more interesting if we consider interacting systems. In particular, following Ref. (Gritsev and Polkovnikov, 2012) we quote the numerical results for the Chern number computed through the

non-adiabatic response for a disordered spin chain:

$$\mathcal{H} = -\vec{h}\sum_{j=1}^{N}\zeta_j\vec{\sigma}_j - J\sum_{j=1}^{N-1}\eta_j\vec{\sigma}_j\vec{\sigma}_{j+1}, \tag{123}$$

where ζ_j and η_j are drawn from a uniform distribution in the interval $[0.75, 1.25]$. We fix the $|\vec{h}| = 1$ and look into the Berry curvature associated with angles of the magnetic field θ and ϕ as a function of J (see Fig. 7). Because of the $SU(2)$ invariance of the system like for a single spin the Chern number and the Berry curvature are simply different by a factor of 2. At large negative J

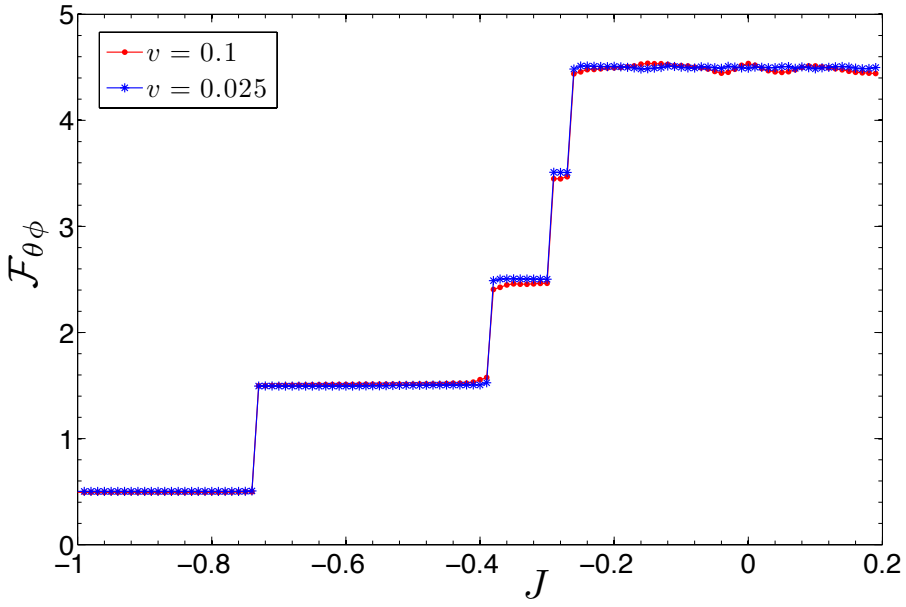

FIG. 7 Berry curvature at the equatorial plain $\theta = \pi/2$ for a disordered spin chain as a function of the coupling J for 9 spins. At large negative J the system minimizes the total spin to $S = 1/2$ the Berry curvature is also $1/2$ corresponding to the Chern number equal to one. At small J the system becomes polarized and the Chern number is 9.

the system minimizes the total spin to $S = 1/2$ the Berry curvature is also $1/2$ corresponding to the Chern number equal to one. At small J the system becomes polarized and the Chern number is 9. In between the Berry curvature and thus the Chern number changes in steps. If one breaks the $SU(2)$ invariance considering e.g. anisotropic interactions the quantization of the Berry curvature disappears while the Chern number remains quantized. The minimal model for observing this is a two-spin system, which was recently realized experimentally also using superconducting qubits (P. Roushan et. al., unpublished).

B. General approach to non-adiabatic response. Emergent Newtonian dynamics.

In this section we extend the analysis of a previous section to a more general class of systems, which are not necessarily in a ground state and which might have gapless excitations. This chapter closely follows Ref. (D'Alessio and Polkovnikov, 2014). Our starting point will be the von Neumann's equation for the density matrix in the moving frame

$$i\frac{d\rho}{dt} = \left[\mathcal{H} - \dot{\lambda}_\nu \mathcal{A}_\nu, \rho\right],$$

where we remind that $\mathcal{H}$ is the diagonal Hamiltonian in the instantaneous basis (we drop the tilde sign to simplify notations), similarly all other observables appearing here are also rotated into the instantaneous frame. We will then use the standard time-dependent perturbation theory (Kubo formalism), where the Galilean term plays the role of the perturbation. Namely we will go to the interaction picture (the Heisenberg representation with respect to $\mathcal{H}$), where the von Neumann's equation becomes

$$i\,\frac{d\rho_H}{dt} = -\dot{\lambda}_\nu \left[\mathcal{A}_{H,\nu}(t), \rho_H\right], \tag{124}$$

which is equivalent to the integral equation

$$\rho_H(t) = \rho_H(0) + i\int_0^t dt' \dot{\lambda}_\nu(t') \left[\mathcal{A}_{H,\nu}(t'), \rho_H(t')\right] \tag{125}$$

Note that if the moving Hamiltonian $\mathcal{H}$ is time dependent if the spectrum explicitly depends on $\vec{\lambda}$. However, this dependence is trivial because it amounts to phase factors $\phi_n = \int_0^t E_n(t')dt'$ instead of $\phi_n = E_n t$. For example

$$\langle\tilde{n}|O_H(\lambda(t))|\tilde{m}\rangle = \exp\left[i\int_0^t dt'(E_n(t') - E_m(t'))\right]\langle\tilde{n}|O(\lambda(t))|\tilde{m}\rangle, \tag{126}$$

where $|\tilde{n}\rangle$ denotes the co-moving basis states. We emphasize that this expression is not the same as the Heisenberg representation with respect to the original Hamiltonian $\mathcal{H}(\lambda(t))$ in the lab frame. The representation we use is perhaps more correctly termed as the adiabatic Heisenberg representation since it uses adiabatic energy levels $E_n(t)$, while all the transitions (off-diagonal terms) are treated perturbatively. Clearly if the spectrum is time independent the expression (126) reduces to the conventional Heisenberg representation of the operator $O(\lambda(t))$. In the leading order in perturbation theory we can substitute the stationary density matrix into the R.H.S. of the integral equation (125):

$$\rho_H(t) = \rho_0 + i\int_0^t dt' \dot{\lambda}_\nu(t') \left[\mathcal{A}_{H,\nu}(t'), \rho_0\right], \tag{127}$$

where we used $\rho_H^0 = \rho^0$. From this we can find the linear response correction to the generalized forces:

$$\langle \mathcal{M}_\nu(t)\rangle = M_\nu(t) + i\int_0^t dt'\,\dot\lambda_\mu(t')\langle[\mathcal{M}_{H,\nu}(t),\mathcal{A}_{H,\mu}(t')]\rangle_0,$$

where we recall that by definition $M_\nu(t)\equiv\langle\mathcal{M}_\nu(t)\rangle_0$. Evaluating this expression in the co-moving basis and using Eqs. (44) and (70) we arrive at

$$\begin{aligned}
\langle \mathcal{M}_\nu(t)\rangle &= M_\nu(t) - \int_0^t dt'\,\dot\lambda_\mu(t')\sum_{n\neq m}\frac{\rho_n^0-\rho_m^0}{E_m-E_n}\mathrm{e}^{i(E_m-E_n)(t-t')}\langle\tilde m|\mathcal{M}_\nu(\lambda(t))|\tilde n\rangle\langle\tilde n|\mathcal{M}_\mu(\lambda(t'))|\tilde m\rangle\\
&= M_\nu(t) - \int_0^t dt'\,\dot\lambda_\mu(t')\sum_{n\neq m}\frac{\rho_n^0-\rho_m^0}{E_m-E_n}\langle\tilde m|\mathcal{M}_{H,\nu}(t)|\tilde n\rangle\langle\tilde n|\mathcal{M}_{H,\mu}(t')|\tilde m\rangle\\
&= M_\nu(t) - \int_0^t dt'\int_0^\beta d\tau\;\dot\lambda_\mu(t')\sum_{n\neq m}\rho_m^0\langle\tilde m|\mathcal{M}_{H,\nu}(t)|\tilde n\rangle\langle\tilde n|\mathcal{M}_{H,\mu}(t'+i\tau)|\tilde m\rangle\\
&= M_\nu(t) - \int_0^t dt'\int_0^\beta d\tau\;\dot\lambda_\mu(t')\langle\mathcal{M}_{H,\nu}(t)\mathcal{M}_\mu(t'+i\tau)\rangle_0,
\end{aligned}\tag{128}$$

which gives the microscopic force in the most general form. To go from the second to the third line in this equation we used that for the thermal distribution, $\rho_m^0 = Z^{-1}\exp[-\beta E_m]$, we have

$$\int_0^\beta d\tau\;\rho_m^0\;e^{-(E_n-E_m)\tau} = \frac{\rho_n^0-\rho_m^0}{E_m-E_n}\tag{129}$$

It is convenient to change the integration variable in Eq. (128) from t' to $t-t'$ and use the fact that in equilibrium the non-equal time correlation functions are translationally invariant in time. Then

$$\begin{aligned}
\langle \mathcal{M}_\nu(t)\rangle \approx M_\nu(t) - \int_0^t dt'\int_0^\beta d\tau\;\dot\lambda_\mu(t-t')\langle\mathcal{M}_{H,\nu}(t')\mathcal{M}_\mu(i\tau)\rangle_0 \approx\\
M_\nu - \int_0^t dt'\dot\lambda_\mu(t-t')\sum_{n\neq m}\frac{\rho_n^0-\rho_m^0}{E_m-E_n}\mathrm{e}^{i(E_m-E_n)t'}\langle m_\lambda|\mathcal{M}_\nu|n_\lambda\rangle\langle n_\lambda|\mathcal{M}_\mu|m_\lambda\rangle
\end{aligned}\tag{130}$$

Now we will use the time scale separation. Namely, recall that by the assumption $\vec\lambda$ represent slow variables in the system. Mathematically this statement implies that the non-equal time correlation function of the generalized forces $\langle\mathcal{M}_{H,\nu}(t')\mathcal{M}_\mu(i\tau)\rangle_0$ decays much faster than the characteristic time scale of changing $\vec\lambda(t)$. Because we are interested in long time dynamics of the system we can extend the upper integration limit over $t-t'$ to ∞ (corresponding to the process starting in the infinite paste). Effectively this corresponds to neglecting short time transients. Because of the time scale separation it is natural to expand $\dot\lambda_\mu(t-t')$ into the Taylor series near $t'=0$: $\dot\lambda_\mu(t-t')\approx\dot\lambda_\mu(t)-t'\ddot\lambda_\mu(t)+\ldots$. As we will see shortly it is important to keep the first two terms

in this expansion and all other terms, in most cases, describe unessential subleading corrections.[5] Then we find

$$\langle \mathcal{M}_\nu(t)\rangle = M_\nu + F_{\nu\mu}\dot{\lambda}_\mu - \eta_{\nu\mu}\dot{\lambda}_\mu - \kappa_{\nu\mu}\ddot{\lambda}_\mu - F'_{\nu\mu}\ddot{\lambda}_\mu, \tag{131}$$

where we split the coefficients in front of $\dot{\lambda}_\mu$ and $\ddot{\lambda}_\mu$ into symmetric $\eta_{\nu\mu}$, $\kappa_{\nu\mu}$ and anti-symmetric $F_{\nu\mu}$ and $F'_{\nu\mu}$ components.

To find the explicit expressions for these coefficients we only need to evaluate simple integrals. First

$$\int_0^\infty \exp[i(E_m - E_n)t']dt' = -iP\left(\frac{1}{E_m - E_n}\right) + \pi\delta(E_n - E_m), \tag{132}$$

where P stands for the principal value. Note that the first principal value term is antisymmetric under the permutation of indexes n and m, while the second is symmetric. Because, as it is evident from Eq. (130), the permutation of n and m is equivalent to the permutation of ν and μ we see that the principal value determines the antisymmetric coefficient $F_{\mu\nu}$ and the second, symmetric term determines $\eta_{\mu\nu}$. Therefore

$$\begin{aligned} F_{\mu\nu} &= -i\sum_{n\neq m}\frac{\rho_n^0 - \rho_m^0}{(E_m - E_n)^2}\langle m_\lambda|\mathcal{M}_\nu|n_\lambda\rangle\langle n_\lambda|\mathcal{M}_\mu|m_\lambda\rangle \\ &= i\sum_{n\neq m}\rho_n^0\frac{\langle m_\lambda|\mathcal{M}_\nu|n_\lambda\rangle\langle n_\lambda|\mathcal{M}_\mu|m_\lambda\rangle - \langle m_\lambda|\mathcal{M}_\mu|n_\lambda\rangle\langle n_\lambda|\mathcal{M}_\nu|m_\lambda\rangle}{(E_n - E_m)^2}. \end{aligned} \tag{133}$$

If we compare this expression with Eq. (71) we will recognize that $F_{\mu\nu}$ is just the thermal average of the Berry curvature over the energy eigenstates. This justifies that we use the same notation $F_{\mu\nu}$ here. At zero temperature this expression obviously reduces to the ground state Berry curvature. Similarly

$$\eta_{\nu\mu} = \pi\beta\sum_{n\neq m}\rho_m^0\langle m_\lambda|\mathcal{M}_\nu|n_\lambda\rangle\langle n_\lambda|\mathcal{M}_\mu|m_\lambda\rangle\delta(E_n - E_m),$$

where we used that

$$\frac{\rho_n^0 - \rho_m^0}{E_m - E_n} \to \rho_n^0\beta \tag{134}$$

when $E_m \to E_n$. As we will see shortly $\eta_{\mu\nu}$ represents the friction force on the system. It is non-zero only if the system has gapless excitation. In particular, at zero temperature, unless the

[5] An important exception is a motion of a charged object in a vacuum, where the friction force is proportional to the third derivative of the coordinate. In this case one has to add the next term to this expansion.

system is quantum critical, the friction coefficient is always zero because one can not satisfy the δ function constraint.

In a similar spirit one can derive the other two coefficients. Now we will use that

$$-\int_0^\infty t' \exp[i(E_m - E_n)t']dt' = \frac{1}{(E_n - E_m)^2} - \pi\delta'(E_n - E_m), \tag{135}$$

which can be checked by adding small imaginary part into the integral and sending it to zero. Now the off-shell term is symmetric, while the on-shell term is antisymmetric. The first off-shell term defines the coefficient $\kappa_{\nu\mu}$, which as we will see shortly determines the mass renormalization

$$\kappa_{\nu\mu} = \sum_{n\neq m} \frac{\rho_n^0 - \rho_m^0}{(\epsilon_m - \epsilon_n)^3} \langle m_\lambda|\mathcal{M}_\nu|n_\lambda\rangle\langle n_\lambda|\mathcal{M}_\mu|m_\lambda\rangle = \sum_{n\neq m} \frac{\rho_n^0 - \rho_m^0}{\epsilon_m - \epsilon_n} \langle m_\lambda|\overleftarrow{\partial_{\lambda_\nu}}|n_\lambda\rangle\langle n_\lambda|\overrightarrow{\partial_{\lambda_\mu}}|m_\lambda\rangle \tag{136}$$

At low temperatures $\beta \to \infty$ this expression reduces to

$$\kappa_{\nu\mu} \approx \sum_{m\neq 0} \frac{\langle 0_\lambda|\mathcal{M}_\nu|m_\lambda\rangle\langle m_\lambda|\mathcal{M}_\mu|0_\lambda\rangle + \nu \leftrightarrow \mu}{(E_m - E_0)^3}, \tag{137}$$

while at high temperatures (or near the classical limit) we find

$$\kappa_{\nu\mu} \approx \frac{\beta}{2} \sum_m \rho_m \left(\langle m_\lambda|\overleftarrow{\partial_{\lambda_\nu}}\,\overrightarrow{\partial_{\lambda_\mu}}|m_\lambda\rangle_c + \nu \leftrightarrow \mu\right) = \beta\, g_{\nu\mu} \tag{138}$$

where $g_{\nu\mu}$ is the Fubini-Study metric tensor of energy eigenstates weighted with the thermal distribution. This is a natural finite temperature generalization of the zero-temperature metric tensor. Let us mention that in traditional units the expressions for the mass Eqs. (136) - (138) should be multiplied by $\hbar^2$, which follows from the correct definition of the Gauge potentials $i\partial_{\lambda_\mu} \to i\hbar\partial_{\lambda_\mu}$. We also point that the mass tensor κ can be written through the integrated connected imaginary time correlation function of the gauge potentials $\mathcal{A}_\nu$ and $\mathcal{A}_\mu$:

$$\kappa_{\nu\mu} = \frac{1}{2}\int_0^\beta d\tau \langle \mathcal{A}_{H,\nu}(-i\tau)\mathcal{A}_{H,\mu}(0) + \nu \leftrightarrow \mu\rangle_{0,c} \tag{139}$$

At high temperatures the imaginary time integral reduces to a factor β and this result clearly reduces to Eq. (138). And finally let us quote the expression for the antisymmetric tensor F':

$$F'_{\mu\nu} = i\pi \sum_{n\neq m} \frac{\rho_n^0 - \rho_m^0}{E_n - E_m} \langle m_\lambda|\mathcal{M}_\nu|n_\lambda\rangle\langle n_\lambda|\mathcal{M}_\mu|m_\lambda\rangle\, \delta'(E_n - E_m) \tag{140}$$

As η this tensor is responsible for dissipation, but usually it is subleading and we will not discuss it further. We only point that as F this tensor is always zero if the instantaneous Hamiltonian respects time-reversal symmetry.

To see that the coefficients found above indeed have a meaning of the mass and the friction we will now assume that $\vec{\lambda}(t)$ is not an external parameter but rather a macroscopic dynamical slow

degree of freedom so that the total Hamiltonian describing the degree of freedom $\vec{\lambda}$ and the rest of the system is

$$\mathcal{H}_{tot}(\vec{\lambda}) = \mathcal{H}_0(\vec{\lambda}) + \mathcal{H}(\vec{\lambda}), \tag{141}$$

where $\mathcal{H}_0(\vec{\lambda})$ is the Hamiltonian describing the bare motion of $\vec{\lambda}$. The choice of splitting $\mathcal{H}_{tot}$ between $\mathcal{H}_0$ and $\mathcal{H}$ is somewhat arbitrary and we can well choose $\mathcal{H}_0 = 0$ so that $\mathcal{H}_{tot} = \mathcal{H}$, however, for an intuitive interpretation of the results, it is convenient to assume that $\mathcal{H}_0(\vec{\lambda})$ represents a massive degree of freedom in some external potential $V(\vec{\lambda})$:

$$\mathcal{H}_0(\vec{\lambda}) = \frac{\vec{p}_\lambda^{\,2}}{2m} + V(\vec{\lambda}).$$

In the infinite mass limit ($m \to \infty$), $\vec{\lambda}$ represents an external (control) parameter whose dynamics is specified a priori. When m is finite, $\vec{\lambda}$ is a dynamical variable and its dynamics needs to be determined self-consistently.

We can now self-consistently combine Eq. (131) with the classical (Lagrangian) equations of motion for the parameter $\vec{\lambda}$:

$$m_{\nu\mu}\frac{d\lambda_\nu}{dt} = p_\nu, \quad \frac{dp_\nu}{dt} = -\frac{\partial V}{\partial \lambda_\nu} + \langle \mathcal{M}_\nu(t) \rangle \tag{142}$$

and get the multicomponent dissipative Newton's equations:

$$(m_{\nu\mu} + \kappa_{\nu\mu} + F'_{\nu\mu})\ddot{\lambda}_\mu + (\eta_{\nu\mu} - F_{\nu\mu})\dot{\lambda}_\mu = -\frac{\partial V}{\partial \lambda_\nu} + M_\nu. \tag{143}$$

The first term in this equation represents the renormalized mass thus $\kappa_{\nu\mu}$ indeed represents the mass renormalization. The term $\eta_{\nu\mu}\dot{\lambda}_\mu$ is clearly dissipative. The Berry curvature defines an analogue of the Coriolis or the Lorentz force and the other antisymmetric on-shell contribution encoded in F' is effectively an antisymmetric friction term. And finally M_ν is the generalized force appearing in e.g. the Born-Oppenheimer approximation. It also defines the Casimir force.

Equation (143) has another interesting implication. At zero temperature both dissipative tensors (η and F') vanish (unless the system is tuned to a critical point or if it has gapless low-dimensional excitations). In this case Eq. (143) can be viewed as a Lagrangian equation of motion with the Lagrangian:

$$\mathcal{L} = \frac{1}{2}\,\dot{\lambda}_\nu\,(m+\kappa)_{\nu\mu}\,\dot{\lambda}_\mu + \dot{\lambda}_\mu\,A_\mu(\vec{\lambda}) - V(\vec{\lambda}) - E_0(\vec{\lambda}), \tag{144}$$

where $A_\mu(\vec{\lambda}) = \langle 0_\lambda|\mathcal{A}_\mu|0_\lambda\rangle$ and $E_0(\vec{\lambda}) = \langle 0_\lambda|\mathcal{H}(\vec{\lambda})|0_\lambda\rangle$ are the value of the Berry connection and Hamiltonian (see Eq. (141)) in the instantaneous ground state. From the Lagrangian (144) we can

define the canonical momenta conjugate to the coordinates λ_ν:

$$p_\nu \equiv \frac{\partial \mathcal{L}}{\partial \dot{\lambda}_\nu} = (m_{\nu\mu} + \kappa_{\nu\mu})\dot{\lambda}_\mu + A_\nu(\vec{\lambda}) \tag{145}$$

and the emergent Hamiltonian:

$$\mathcal{H}_\lambda \equiv \dot{\lambda}_\nu\, p_\nu - \mathcal{L} = \frac{1}{2}(p_\nu - A_\nu)(m+\kappa)^{-1}_{\nu\mu}(p_\mu - A_\mu) + V(\vec{\lambda}) + E_0(\vec{\lambda}). \tag{146}$$

Clearly the Berry connection term plays the role of the vector potential. Thus we see that the whole formalism of the Hamiltonian dynamics for arbitrary macroscopic degrees of freedom is actually emergent. Without the mass renormalization this (minimal coupling) Hamiltonian was first derived in Ref. (Berry, 1989). Away from the ground state the dissipative tensors (η and F') are, in general, non-zero and it is not possible to reformulate Eq. (143) via Hamiltonian dynamics.

Let us illustrate this formalism with two simple examples. First we consider a massless spring connected to the potential wall. In this section we will explicitly insert all factors of $\hbar$. We also imagine that a quantum particle of mass m is initially prepared in the ground state of the confining potential (see the left panel in Fig. 8). As in the previous example we will compute how the mass of a classical object (the spring) coupled to a quantum environment (the potential well) is renormalized.

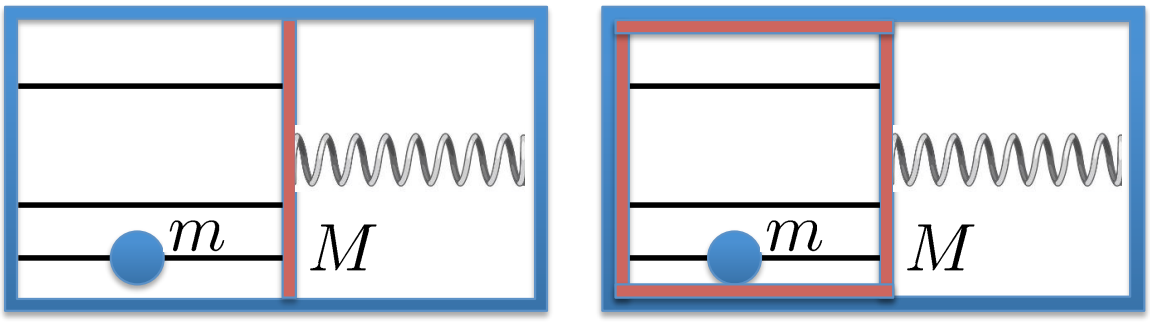

FIG. 8 (Color on-line) Schematic of a quantum piston. a) The spring is connected to a wall of the potential in which a quantum particle of mass m is initially confined into the ground state. b) As in a) but now the spring is connected to the whole potential well which moves rigidly. The wave-lines in a) and b) represent the low energy wavefunctions of the quantum particle in the confining potential.

According to Eq. (137) the mass renormalization is given by

$$\kappa_R = 2\hbar^2 \sum_{n\neq 0} \frac{|\langle n_\lambda|\mathcal{M}|0_\lambda\rangle|^2}{(E_n - E_0)^3}, \tag{147}$$

where $\lambda = X_R$ is the position of the right potential wall. We approximate the confining potentail

as a very deep square well potential. Then $\mathcal{M} \equiv -\partial_\lambda \mathcal{H} = -V\delta(x - X_R)$ and we find

$$\kappa_R = 2\hbar^2 \sum_{n\neq 0} \frac{V^2 |\psi_0(X_R)|^2 |\psi_n(X_R)|^2}{(E_n - E_0)^3}. \tag{148}$$

Using the well known result for a finite (and deep) square well potentail

$$|\psi_n(X_R)| = \sqrt{\frac{2}{L}}\,\sqrt{\frac{E_n}{V}}$$

where the factor of $\sqrt{2/L}$ comes from the normalizazion of the wave-function in a square potential of length L, we obtain

$$\kappa_R = 2\hbar^2 \left(\frac{2}{L}\right)^2 \sum_{n\neq 0} \frac{E_0 E_n}{(E_n - E_0)^3}. \tag{149}$$

Substituting

$$E_n = \frac{\hbar^2 k_n^2}{2m}, \quad k_n = \frac{n+1}{L}\,\pi, \quad \forall n \geq 0$$

we arrive at

$$\kappa_R = m\,\frac{16}{\pi^2} \sum_{n\geq 1} \frac{(n+1)^2}{[(n+1)^2 - 1]^3} = m\,\frac{2\pi^2 - 3}{6\pi^2} \approx 0.28m$$

The result is identical if we connect the piston to the left wall, i.e. $\kappa_L = \kappa_R$.

Now let us consider a slightly different setup where the spring connects to the whole potential well (see the right panel in Fig. 8) so that λ now indicates the center of mass of the well. From the Galilean invariance we expect $\kappa = m$. In fact, since now both potentials walls are moving, our expression gives

$$\mathcal{M}_\lambda = -\partial_\lambda \mathcal{H} = -V(\delta(x - X_R) - \delta(x - X_L)),$$

where X_L and X_R are the left and right positions of the walls. Thus using Eq. (147) we obtain

$$\kappa_+ = 2\hbar^2 \sum_{n\neq 0} \frac{V^2 (\psi_0(X_L)\psi_n(X_L) - \psi_0(X_R)\psi_n(X_R))^2}{(E_n - E_0)^3} \tag{150}$$

Since in a symmetric potential well $\psi_n(X_R) = (-1)^n \psi_n(X_L)$ only the odd terms contribute in the equation above. Following the same line of reasoning as before we arrive at (note the extra factor of 4 with respect to Eq. (149))

$$\kappa_+ = 2\hbar^2 \left(\frac{2}{L}\right)^2 4 \sum_{n=odd} \frac{E_0 E_n}{(E_n - E_0)^3} = m\frac{64}{\pi^2} \sum_{n=odd} \frac{(n+1)^2}{[(n+1)^2 - 1]^3} = m$$

So indeed we recover the expected result. This simple calculation illustrates that we can understand the notion of the mass as a result of virtual excitations created due to the acceleration of the external coupling (position of the wall(s) in this case). If instead we analyze the setup where the two walls are connected to a spring and move towards each other so that λ is the (instantaneous) length of the potential well we find

$$\begin{aligned}\kappa_- &= 2\hbar^2 \sum_{n\neq 0} \frac{V^2(\psi_0(X_L)\psi_n(X_L) + \psi_0(X_R)\psi_n(X_R))^2}{(E_n - E_0)^3} \\ &= m\frac{64}{\pi^2} \sum_{\substack{n=even \\ n\neq 0}} \frac{(n+1)^2}{[(n+1)^2-1]^3} = m\frac{\pi^2-6}{3\pi^2} \approx 0.13m.\end{aligned} \tag{151}$$

Let us point another peculiar property of the mass. Clearly $\kappa_L + \kappa_R \approx 0.56m \neq \kappa_+, \kappa_-$, i.e. the mass renormalization of the two walls is not the same as the sum of the mass renormalization of each wall measured separately. This is a result of quantum interference, which is apparent in Eqs. (150) and (151). Note that $(\kappa_+ + \kappa_-)/2 = \kappa_L + \kappa_R$. Thus the mass behaves similarly to the intensity in the double pass interferometer, where the sum of intensities in the symmetric and antisymmetric channels is conserved. At a high temperature or in the classical limit the interference term will disappear and we will find $\kappa_L = \kappa_R \approx 0.5m$.

As a second example let us consider a macroscopic rotator (angular momentum) interacting with independent spin-$\frac{1}{2}$ particles. If instead of the rotator we use the quantum spin operator, this model is known as the central spin model. Because dynamics of a spin in any external field is always classical (the evolution of the Wigner function is exactly described by classical trajectories) there is no difference between quantum and classical dynamics in this case and we do not need to assume that the rotator is macroscopic. The Hamiltonian describing the system is (141) with

$$\mathcal{H}_0 = \frac{\vec{L}^2}{2I} + V(\vec{n}), \quad \mathcal{H} = -\vec{n}\cdot\sum_{i=1}^{N} \Delta_i \vec{\sigma}_i, \tag{152}$$

where I is the momentum of inertia, $V(\vec{n})$ is a time-dependent external potential, $\vec{L}$ is the angular momentum and $\vec{n}$ is the three-dimensional unit vector which can be parameterized using spherical angles: $\vec{n} = (n_x, n_y, n_z) = (\sin\theta\cos\phi, \sin\theta\sin\phi, \cos\theta)$. This example is similar to the one considered earlier except that the effective magnetic field is no longer confined to the xz plane and we no longer assume that it is given by an external protocol. The time evolution of this system needs to be found self-consistently. On the one hand, each spin evolves according to the von Neumann equation with the time-dependent Hamiltonian $\mathcal{H}(\vec{n}(t))$:

$$i\partial_t \rho = [\mathcal{H}(\vec{n}(t)), \rho] \tag{153}$$

and, on the other hand, the rotator evolves according to the Hamilton equations of motion

$$I\dot{\vec{n}} = \vec{L} \times \vec{n}, \quad \dot{\vec{L}} = \vec{n} \times \left(\vec{M}_{ext} + \langle -\frac{\partial \mathcal{H}}{\partial \vec{n}} \rangle \right) = \vec{n} \times \left(\vec{M}_{ext} + \sum_i \Delta_i \langle \vec{\sigma}_i \rangle \right) \tag{154}$$

where $\vec{M}_{ext} = -\frac{\partial V(\vec{n})}{\partial \vec{n}}$ is the external force and $\langle \dots \rangle$ indicates the quantum average over the density matrix $\rho(t)$ (see Eq. (153)). We assume that initially $\vec{n}_0 = (0, 0, 1)$ and the spins are in thermal equilibrium with respect the Hamiltonian $\mathcal{H}(\vec{n}_0)$, i.e. $\langle \sigma_i^x \rangle_0 = \langle \sigma_i^y \rangle_0 = 0$ and $\langle \sigma_i^z \rangle_0 = \tanh(\beta \Delta_i)$.

For the toy model proposed here these coupled equations can be easily solved numerically. In fact, according to the Ehrenfest theorem, the evolution of the expectation values follow the classical equation of motion and the von Neumann equation (153) can be replaced with the much simpler equation $\dot{\vec{m}}_i = 2\Delta_i \, \vec{m}_i \times \vec{n}$ where $\vec{m}_i = \langle \vec{\sigma}_i \rangle$. Therefore the exact dynamics of the system consists of the vectors $(\vec{L}, \vec{n}, \{\vec{m}_i\})$ precessing around each other.

We now compare the exact dynamics with the emergent Newton's law. First, we note that the form of Eqs (154) immediately implies

$$\begin{aligned} &\dot{\vec{n}} \cdot \vec{L} = 0, \ \vec{n} \cdot \dot{\vec{L}} = 0 \to \vec{n} \cdot \vec{L} = \text{const} \\ &\dot{\vec{n}} \cdot \vec{n} = 0 \to |\vec{n}|^2 = \text{const}, \ \ddot{\vec{n}} \cdot \vec{n} = -|\dot{\vec{n}}|^2 \end{aligned} \tag{155}$$

Next we need to compute the generalized force $\langle \vec{\mathcal{M}} \rangle = -\langle \partial_{\vec{n}} \mathcal{H} \rangle$, and the tensors κ and F. The drag term η and the anti-symmetric mass F' are zero since there are no gapless excitations. Therefore Eq. (131) reduces to:

$$\langle \vec{\mathcal{M}} \rangle = \langle \vec{\mathcal{M}} \rangle_0 + F_{\nu,\mu} \dot{n}_\mu - \kappa_{\nu,\mu} \ddot{n}_\mu$$

where $\nu, \mu = x, y, z$. The ground and excited states of each spin-$\frac{1}{2}$ are:

$$|gs^i_{\theta,\phi}\rangle = \begin{pmatrix} \cos\left(\frac{\theta}{2}\right) \mathrm{e}^{-i\phi/2} \\ \sin\left(\frac{\theta}{2}\right) \mathrm{e}^{+i\phi/2} \end{pmatrix}, \quad |ex^i_{\theta,\phi}\rangle = \begin{pmatrix} \sin\left(\frac{\theta}{2}\right) \mathrm{e}^{-i\phi/2} \\ -\cos\left(\frac{\theta}{2}\right) \mathrm{e}^{+i\phi/2} \end{pmatrix} \tag{156}$$

with energy $\pm\Delta_i$ respectively from which it follows

$$\langle \vec{\mathcal{M}} \rangle_0 = 0, \quad F = F_0 \begin{pmatrix} 0 & n_z & -n_y \\ -n_z & 0 & n_x \\ n_y & -n_x & 0 \end{pmatrix},$$

$$\kappa = \kappa_0 \begin{pmatrix} 1 - n_x^2 & -n_x n_y & -n_x n_z \\ -n_y n_x & 1 - n_y^2 & -n_y n_z \\ -n_z n_x & -n_z n_y & 1 - n_z^2 \end{pmatrix}.$$

where $F_0 \equiv \frac{1}{2}\sum_i \tanh(\beta\Delta_i)$ and $\kappa_0 \equiv \sum_i \frac{\tanh(\beta\Delta_i)}{4\Delta_i}$. Substituting these expressions in Eq. (154) we find

$$I\dot{\vec{n}} = \vec{L}\times\vec{n},\ \dot{\vec{L}} = \vec{n}\times\vec{M}_{ext} + F_0\,\dot{\vec{n}} - \kappa_0\,(\vec{n}\times\ddot{\vec{n}})$$

where we have used standard properties of the vector triple product together with Eqs. (155). In the equations above we can substitute $\vec{L}\to\vec{L}_\perp$ where by definition $\vec{L}_\perp = \vec{L} - (\vec{L}\cdot\vec{n})\vec{n}$. We now compute $I\ddot{\vec{n}} = \dot{\vec{L}}_\perp\times\vec{n} + \vec{L}_\perp\times\dot{\vec{n}}$ and using standard properties of the vector triple product together with $\vec{L}_\perp = I\,(\vec{n}\times\dot{\vec{n}})$ and Eqs. (155) we arrive at:

$$I_{eff}\ddot{\vec{n}} = \left(\vec{n}\times\vec{M}_{ext}\right)\times\vec{n} + F_0(\dot{\vec{n}}\times\vec{n}) - I_{eff}|\dot{\vec{n}}|^2\vec{n} \tag{157}$$

where we have defined the renormalized momentum of inertia is $I_{eff} = I + \kappa_0$.

From this equation we see that the moment of inertia of the rotator is renormalized by the interaction with the spin-$\frac{1}{2}$ particles. Moreover we see that, even when the external force is absent ($\vec{M}_{ext} = 0$), the Berry curvature (F_0) causes the Coriolis type force tilting the rotation plane of the rotator. Indeed if we start with uniform rotations of the rotator in the xz plane, i.e. $\vec{n}$, $\dot{\vec{n}}$ lie in the xz plane, we immediately see that the Berry curvature causes acceleration orthogonal to the rotation plane. The physics behind the Coriolis force is intuitively simple. At any finite rotator's velocity, the spins will not be able to follow adiabatically the rotator and thus will be somewhat behind. As a result there will be a finite angle between the instantaneous direction of the spins and the rotator so the spins will start precessing around the rotator. This precession will result in a finite tilt of the spin orientation with respect to the rotation plane proportional to the Berry curvature (as we discussed in the previous section). In turn this tilt will result in precession of the rotator around the spins and cause the tilt of the rotation plane. It is interesting that despite the motion of the rotator is completely classical the Coriolis force given by the Berry curvature is quantum in nature. In particular, at zero temperature the integral of the Berry curvature over the closed manifold (4π spherical angle is this case) is quantized. Therefore by measuring the Coriolis force and averaging it over the angles θ and ϕ one should be able to accurately see a quantized value:

$$\int_0^\pi d\theta \int_0^{2\pi} d\phi\, F_{\theta,\phi} = 2\pi N. \tag{158}$$

It is interesting that this result remains robust against any small perturbations in the system, which do not close the gap in the spectrum. Similarly the origin of the extra mass (moment of inertia) κ in this simple example is purely quantum, i.e. despite this mass describes the classical Newtonian motion, it can not be computed within the classical framework.

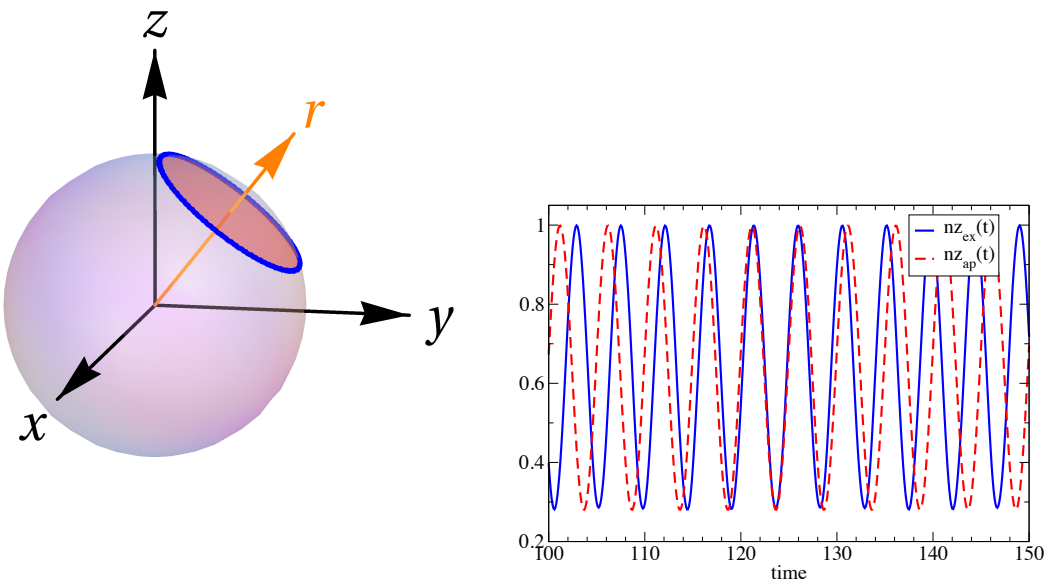

FIG. 9 Dynamics of a rotator coupled to $N = 20$ spins-$\frac{1}{2}$. (Left panel) The exact trajectory of the rotator obtained by numerically solving Eq. (153) and (154) (blue line) coincides with the approximated trajectory Eq. (159) which delimits the shaded red plane. (Right panel) Behavior of $n_z(t)$ for the exact (continuous blue) and approximated evolution (dashed red) versus time. The parameters of the exact simulations are: $N = 20$, $\beta = 0.1$, $I = 1$, Δ_i are randomly distributed in $(1, 2)$. For these parameters $F_0 \approx 1.5$, $\kappa_0 \approx 0.5$ and $I_{eff}/I \approx 1.5$. The initial conditions are $\vec{n}_0 = (0, 0, 1)$ and $\vec{L}_0 = (0, 0, 0)$ and initially the spins are in thermal equilibrium (see main text). We chose the time-dependent external force to be $\vec{M}_{ext}(t) = 250 \left[\frac{t}{t_c}\left(1 - \frac{t}{t_c}\right)\right]^4 \hat{x}$ for $0 \leq t \leq t_c = 3$ and zero otherwise.

We now analyze the approximated Equation (157) in detail. We consider the situation in which $\vec{M}_{ext}(t)$ is slowly turned on (off) at time $t = 0$ ($t = t_c$). When $\vec{M}_{ext}(t) = 0$ Eq. (157) describes a uniform circular motion whose solution can be written as:

$$\vec{n}_{ap}(t) = \sqrt{1 - A_{ap}^2}\ \hat{r} + A_{ap}\ \left[\cos(\omega_{ap} t + \phi)\ \hat{c}_1 + \sin(\omega_{ap} t + \phi)\ \hat{c}_2\right] \tag{159}$$

where A_{ap} is the amplitude, ω_{ap} is the angular frequency, $\hat{r}$ is the vector orthogonal to the plane of motion (see Fig. 9) and $\hat{c}_1$, $\hat{c}_2$ are two orthogonal unit vectors spanning the plane of motion. Substituting the ansatz (159) in Eq. (157) (with $\vec{M}_{ext} = 0$) we obtain

$$\omega_{ap} = -\frac{F_0}{I_{eff}\sqrt{1 - A_{ap}^2}}. \tag{160}$$

The amplitude and the orientation of the plane of motion can not be computed from the initial conditions of Eq. (157) since this equation is only valid after a transient time. We therefore extract

them from the exact numerical solution:

$$\sqrt{1-A_{ap}^2}\,\hat{r} = \lim_{T\to\infty}\frac{1}{T}\int_{t_c}^{t_c+T} dt'\,\vec{n}_{ex}(t')$$

and compute ω_{ap} via Eq. (160). In Fig. 9 we compare the exact trajectory $\vec{n}_{ex}(t)$ obtained by numerically solving Eq. (153) and Eq. (154) for the rotator coupled to $N = 20$ spins with gaps Δ_i uniformly distributed between $(1, 2)$ to the approximated trajectory $\vec{n}_{ap}(t)$ (159). We note that the frequency of the approximated motion (estimated via Eq.(160)) underestimates the exact frequency by 8% however if we had used the bare momentum of inertia in (160) with the chosen simulation parameters ($I_{eff}/I \approx 1.5$) we would have overestimated the exact frequency by 28%. The accuracy will be higher if we increase the number of spins N.

Acknowledgments

These notes were partially based on works done jointly with L. D'Alessio, V. Gritsev, M. Kolodrubetz and P. Mehta.

References

Berry, M. V., 1984, Proceedings of the Royal Society of London. A. Mathematical and Physical Sciences **392**(1802), 45, URL `http://rspa.royalsocietypublishing.org/content/392/1802/45.abstract`.

Berry, M. V., 1989, in *The quantum phase, five years after in "Geometric Phases in Physics", eds: A Shapere, F Wilczek* (World Scientific), pp. 7–28.

Campos Venuti, L., and P. Zanardi, 2007, Phys. Rev. Lett. **99**, 095701.

D'Alessio, L., and A. Polkovnikov, 2014, arXiv:1309.6354 .

Damle, K., and S. Sachdev, 1996, Physical Review Letters **76**(23), 4412, URL `http://link.aps.org/doi/10.1103/PhysRevLett.76.4412`.

Gritsev, V., and A. Polkovnikov, 2012, Proc. Nat. Acad. USA **109**, 6457.

Haldane, F. D. M., 1988, Phys. Rev. Lett. **61**, 2015.

Kolodrubetz, M., V. Gritsev, and A. Polkovnikov, 2013, Phys. Rev. B **88**, 064304.

Kreyszig, E., 1959, *Differential Geometry* (University of Toronto Press, Toronto).

Landau, L., and E. Lifshitz, 1982, *Mechanics: Course of Theoretical Physics Vol. 1* (Butterworth-Heinemann).

Provost, J., and G. Vallee, 1980, Comm. Math. Phys. **76**(3), 289.

Sachdev, S., 1999, *Quantum Phase Transitions* (Cambridge University Press).